2013-07-08

Nuclear BMP2 and the Immune Response

Daniel S. Olsen
Brigham Young University - Provo

Nuclear BMP2 and the Immune Response

Daniel S. Olsen

A thesis submitted to the faculty of
Brigham Young University
in partial fulfillment of the requirements for the degree of

Master of Science

Laura Bridgewater, Chair
Jeffery Barrow
Julianne Grose

Department of Microbiology and Molecular Biology

Brigham Young University

July 2013

ABSTRACT

Nuclear BMP2 and the Immune Response

Daniel S. Olsen
Department of Microbiology and Molecular Biology, BYU
Master of Science

Nuclear bone morphogenetic protein 2 (nBMP2) is a nuclear variant of the secreted growth factor BMP2. Experiments in nBmp2NLS^{tm} mutant mice, which lack nBMP2 in the nucleus, have shown that nBMP2 affects intracellular calcium transport in skeletal muscle and hippocampal neurons. The objective of this study was to determine whether nBMP2 affects the immune system, since activation of lymphocytes and other immune cells depends on intracellular calcium transport. We found that spleens in nBmp2NLS^{tm} mutant mice were 24% smaller than in wild type mice. The white pulp of the spleen contains many immune cells, particularly B and T lymphocytes and reduced spleen size in the nBmp2NLS^{tm} mutant mice could be caused by a reduced number of lymphocytes migrating to the spleen.

When mutants and wild types were challenged with an intravenous infection of 10^7 CFU of *S. aureus*, they showed similar immune responses. Samples of blood, liver, spleen, kidney and lymph nodes cultured three days after infection showed no difference in post infection bacterial load between mutant and wild type. Likewise, post-infection weight loss and percent survival were similar between mutant and wild type, suggesting that the innate immune response is functional in nBmp2NLS^{tm} mice. However, when mice were challenged with a secondary infection, immune response and spleen function were severely impaired. Mutant mice showed higher levels of bacteria remaining in the blood and had lower rate of survival to day 3 after secondary infection. In addition, $CD4^+$ and $CD8^+$ T-cell levels within mutant lymph nodes were significantly reduced, indicating that nBMP2 is involved in the secondary immune response.

Keywords: BMP2, calcium transport, immunology, infection, lymphocytes, nuclear localization, spleen function, T-cells

ACKNOWLEDGEMENTS

There are many people who have assisted in one way or another to make this work possible. I would like to thank my advisor, Dr. Laura Bridgewater, for her help and feedback with conducting this project as well as writing this thesis. I am grateful to my graduate committee members, Dr. Jeffery Barrow and Dr. Julianne Grose, for their encouragement and feedback on the progress of this project. In addition, I would like to thank Dr. Scott Weber for his help and encouragement, particularly with the lymphocyte identification experiments. I am grateful to Nelson Laboratories for providing me with a work schedule flexible enough to accommodate graduate school. The microbiological testing experience I have gained there was also key to the successful completion of this project.

Life's endeavors are truly only as good as the people by whom you are surrounded. I am very grateful to my lab mates in the Bridgewater Lab for helping to make this project a fun and memorable experience. In particular, I thank fellow graduate student Brandt Nichols for his friendship, feedback, and constant willingness to help. I am grateful for my family, especially my beautiful wife, Ashley, for her unending love and support. Lastly, I would like to thank my daughter, Makay, for brightening even the most stressful days with her smile.

TABLE OF CONTENTS

LIST OF TABLES

LIST OF FIGURES

INTRODUCTION

Nuclear bone morphogenetic protein 2 (nBMP2) is a recently discovered nuclear variant of the secreted growth factor bone morphogenetic protein 2 (BMP2) [1]. nBMP2 is synthesized from the same gene and same mRNA transcript as the secreted BMP2. Because of this, it is possible that some of the functions that have been attributed to BMP2 are actually carried out by nBMP2. There is, therefore, a great need to characterize the specific functions of nBMP2 in order to differentiate them from those of the secreted BMP2.

Bone morphogenetic proteins (BMPs) are members of the transforming growth factor β (TGF-β) superfamily of growth factors. The TFG-β superfamily has many subfamilies, including BMPs and growth differentiation factors [2]. Over twenty BMP family members have been identified and characterized, making BMPs the largest subfamily of the TGF-β superfamily. BMPs are involved in many different developmental pathways, including axis formation, limb patterning, heart development, neural crest cell migration, neurogenesis, and apoptosis [3]. BMP2 plays an important role in the development of bone, cartilage and heart, as well as directing the development of neural crest cells [4, 5].

BMP2, like other members of the TGF-β superfamily, is first produced as a preproprotein, including an N-terminus signal peptide which directs it to the endoplasmic reticulum (ER) for processing as part of the secretory pathway. During this process, the proprotein is cleaved by proprotein convertases, releasing the C-terminal peptide. The C-terminal peptide homodimerizes to form the mature secreted growth factor. nBMP2 is produced by alternative translation of the BMP2 mRNA transcript. Alternative translation begins at a downstream start codon, bypassing the signal peptide and thereby avoiding the processing and

cleavage involved with the secreted BMP2. As a result, a nuclear localization signal (NLS) found within the site of cleavage is left intact, directing nBMP2 to be translocated from the cytoplasm to the nucleus.

A line of viable mice bearing a targeted inactivation of nBmp2 (nBmp2NLS^{tm}) has been successfully created. This line was created by targeted mutagenesis of the NLS, thereby preventing BMP2 from translocating to the nucleus even when translation begins from the alternative start site. While Bmp2 null mice are nonviable, displaying fatal defects in amnion/chorion and cardiac development [5], nBmp2NLS^{tm} mice are viable and fertile. Extensive examination of nBmp2NLS^{tm} mice has shown no difference in cartilage and bone formation compared to wild type mice, indicating that function of the secreted BMP2 has not been altered. Although nBmp2NLS^{tm} mice are viable and fertile, they do display abnormal phenotypes compared to wild type mice, including impaired learning and memory along with abnormal muscle contraction and relaxation [6, 7].

In studies testing memory and learning, mutant mice showed greater difficulty in adapting acquired memory to environmental changes, and reduced recognition of novel objects. They also showed reduced long-term potentiation, one of the primary cellular mechanisms mediating learning and memory. These phenotypes are similar to those of ryanodine receptor type 3 (RyR3) knockout mice [8]. In addition to these altered cognitive phenotypes, mutant mice also showed decreased skeletal muscle relaxation rates and decreased sarco/endoplasmic reticulum Ca^{2+} ATPase (SERCA) activity. Both RyR3 and SERCA are calcium transporters heavily involved in regulating intracellular calcium levels. These results indicate that lack of nuclear localized BMP2 leads to dysregulation of intracellular calcium transport.

In addition to its involvement in cognitive function and muscle contraction, intracellular calcium transport is also a key component in the activation and differentiation signaling pathways of many immune cells, including T-cells, B-cells, dendritic cells and macrophages [9-11]. In general, the activation of immunoreceptors on the cell surface triggers a series of protein tyrosine kinase cascades that result in increases in intracellular concentration of Ca^{2+}. This is largely mediated by activation of inositol-1,4,5-trisphosphate (IP_3), which then binds to its receptor (IP_3R) in the endoplasmic reticulum (ER) membrane, causing a rapid release of Ca^{2+} from ER stores into the cytosol [10, 12]. There are also various calcium channels in the cell membrane, referred to as store-operated calcium channels (SOCC), which are activated by depletion of ER calcium stores. Calcium stores in the ER are replenished primarily through SERCA, which has been shown to have decreased activity in muscle of nBmp2NLS^{tm} mutant mice. It is therefore possible that lack of nBMP2 could have a similar effect on the intracellular calcium transport function of lymphocytes and other immune cells. This would result in a reduced ability of nBmp2NLS^{tm} mutant mice to mount an appropriate immune response.

The purpose of this work was to determine the effect of nBMP2 on the immune response to a systemic bacterial infection. Lack of nBMP2 is shown to result in impaired spleen function as well as reduced T-cell levels within lymph nodes, leading to a disrupted immune response to secondary infection.

MOUSE INFECTION STUDIES

Overview

In order to determine whether nBMP2 plays a role in the immune response to bacterial infection, nBmp2NLS$^{tm\ +/+}$ (wild type) and nBmp2NLS$^{tm\ -/-}$ (mutant) mice were infected with *S. aureus* by intravenous injection through the tail vein. Mice were divided into groups to be analyzed at various points in infection. Uninfected controls were injected with 200 μL of sterile PBS and examined 3 days later. Figure 1 shows the experimental setup for primary and secondary infections.

With each group of mice infected, the inoculum concentration was kept constant and the injection volume was varied from 150 – 250 μL, depending on individual mouse weight, to ensure that each mouse received the proper dose. For primary infections, a dose of 3×10^5 CFU/g was administered for mice that were to be analyzed 3 days after infection and a dose of 1×10^4 CFU/g was given to mice that were to be analyzed at 8 days after infection. For secondary infections, a dose of 1×10^4 CFU/g was administered and followed by a secondary injection, 35 days later, of 3×10^5 CFU/g. Inoculum concentration was verified on each day of injections by standard plate count.

Mice were monitored for up to eight days after primary infections and three days after secondary infection. A pain and distress score for the categories of weight loss, appearance, clinical signs and unprovoked behavior was assigned each day of monitoring. Samples were obtained on the day indicated for each group and response to the infection was measured by post-infection bacterial load, lymphocyte distribution, histology and hematology.

Mouse Colony Maintenance

Heterozygous nBmp2NLS^{tm} mice were bred in the Brigham Young University specific pathogen free (SPF) animal facility. After weaning, mice were genotyped and transferred to the non-SPF animal care facility where they were housed and maintained throughout the duration of the study. All mice were given a standard chow and water diet *ad libitum* and kept in a temperature-controlled (21-22°C) room with a 12:12 hour light:dark cycle. Experiments were performed with mice between the ages of 6-8 months. All experiments were performed in accordance with approved Institutional Animal Care and Use Committee (IACUC) protocol.

Bacterial Culture Maintenance

S. aureus, ATCC strain 12600, was obtained from the Microbiology and Molecular Biology department stockroom as a broth culture in tryptic soy broth. Organism identification was verified through morphology, Gram stain, catalase test, and mannitol fermentation. Subsequent passages were created by alternating between a standard streak plate and a broth culture. Streak plates were performed on Mannitol Salt Agar (Alpha Biosciences) and broth cultures were prepared in LB Broth (BD Biosciences). All cultures were incubated for 24 hours at 37°C and stored at 4°C. Broth cultures were placed on a rotating platform at 120 rpm during incubation. Culture titer was determined regularly by standard plate count.

Tail Vein Injections

Prior to performing injections, mice were warmed in an empty cage on a heat pad to dilate the tail vein. The *S. aureus* culture was diluted to desired concentration in phosphate

buffered saline (PBS). Mice were placed in a restrainer and injection solution, either bacterial culture or sterile PBS, was injected using a 1 mL syringe and a 27 gauge needle. Injection dose was verified following injection by standard plate count.

Tissue Preparation

Mice were euthanized by CO_2 inhalation followed by cervical dislocation. Blood samples were taken by cardiac puncture and placed in PBS containing ethylenediaminetetraacetic acid (EDTA) at a final concentration of 1.8 mg/mL to prevent clotting. Mice were then dissected to obtain liver, kidney, spleen and inguinal lymph node samples. Solid tissue samples were weighed, placed in PBS (5-10 mL for liver, spleen and kidney samples; 3-5 mL for lymph node samples) and homogenized using a dounce homogenizer.

Post-Infection Bacterial Load

Tissue samples were serially diluted in ten-fold increments (0.5 mL into 4.5 mL) using PBS as needed to get colony counts within countable range. 100 μL aliquots were plated in triplicate on MSA to select for growth of *S. aureus*. Plates were incubated for 24-48 hours at 37°C. Bacterial load was calculated as CFU/mL for blood samples and CFU/g for solid tissue samples.

Flow Cytometry

Mice were dissected to obtain spleen, thymus and lymph node (inguinal, mesenteric, and lumbar) samples. Tissues were ground using frosted microscope slides and filtered through 70 μm nylon mesh (BD Biosciences) to prepare single cell suspension in PBS. Cells were

centrifuged and resuspended in 5 mL of red blood cell lysis buffer (388 mM NH_4Cl, 29.7 mM $NaHCO_3$, 25 μM Na_2EDTA) for 5 minutes. After red blood cell lysis, samples were centrifuged and resuspended in 500 μL of PBS. In order to reduce non-specific binding of the antibodies, an FC receptor block was performed by adding anti-mouse CD16/32 antibody to cells (1 μL Ab per 100 μL of cells) and incubating at room temperature for 15 minutes. Samples were centrifuged and resuspended in antibody staining solution (1 μL antibody in 200 μL PBS) for 30 minutes. Refer to Table 1 for antibody grouping. All antibodies used were from eBiosciences. Following staining, samples were rinsed once with PBS and measured on a FACSCanto Flow Cytometer (BD Biosciences). Results were analyzed using Summit Software v4.3 (Beckman Coulter) and FlowJo v10.0.6 (Tree Star).

Histology

Spleen samples were fixed overnight in 4% paraformaldehyde in PBS at 4°C. After paraformaldehyde fixation, samples were dehydrated using increasing concentrations of ethanol and processed in a Citadel 1000 tissue processor. Refer to Table 2 for details of the processing cycle. Samples were then embedded in paraffin wax and 5-7 μm sections were prepared. Sections were stained using hematoxylin and eosin (H&E) (Table 3) and observed on a Zeiss Imager A.1 brightfield microscope.

Hematology

To determine red blood cell count, 10 μL of blood was added to 990 μL 1.5 mg/mL EDTA in PBS. Additional dilutions were performed as needed in PBS to get cells in countable range. Cells were counted on a hemocytometer.

To determine white blood cell count, 10 µL of blood was added to 190 µL RBC Lysis Buffer (388 mM NH_4Cl, 29.7 mM $NaHCO_3$, 25 µM Na_2EDTA). Sample was mixed and allowed to sit for 5 minutes. Cells were counted on a hemocytometer.

IDENTIFICATION OF NBMP2 BINDING PARTNERS

Overview

In order to identify potential binding partners of nBMP2 and better understand the role it plays inside the nucleus, co-immunoprecipitation (Co-IP) and mass spectrometry experiments were performed. Using site-directed mutagenesis, versions of nBmp2 containing FLAG, Myc and HA tags were created. Human embryonic kidney 293 (HEK-293) cells were transfected with the tagged versions of nBmp2, followed by co-immunoprecipitation and mass spectrometry analysis.

Site-Directed Mutagenesis

Tagged versions of nBmp2 were prepared by site directed mutagenesis using a QuikChange® II Site-Directed Mutagenesis Kit (Stratagene) to alter the rat nBmp2 gene contained on a pcDNA3.1 plasmid. FLAG, Myc and HA tag sequences were inserted either upstream or downstream of the gene so that they were present at either the N- or C-terminus of the expressed protein. A linker sequence of five glycine residues was inserted between the tag and the gene sequence to reduce allosteric interference and improper protein folding that are possible when adding a tag sequence to a protein. The primers used for each of the tagged versions are shown in Table 4.

After mutagenesis was complete, plasmids were purified from the mutagenesis samples using a GenElute™ Plasmid Miniprep Kit (Sigma). Samples were then sequenced in the Brigham Young University DNA Sequencing Center to verify proper insertion and orientation of tags. Plasmids containing properly inserted tags were transformed into *E. coli* cells and purified using a Plasmid Midi Kit (QIAGEN).

Cell Culture

HEK293 cells were grown in Dulbecco's Modification of Eagle's Medium / Ham's F12 50/50 Mix (Corning cellgro), supplemented with 10% fetal bovine serum and 1% L-Glutamine (Hereafter referred to as DMEM/F12). Cells were grown in 75 cm^2 tissue culture flasks (Sarstedt) and were regularly passaged every 3-4 days. All incubation was performed at 37°C and 5% CO_2.

Immunofluorescent Staining of Cultured Cells

To verify endogenous expression of nBmp2 in HEK293 cells, immunofluorescent staining was performed. HEK293 cells were seeded (5×10^4 cells in 0.5 mL DMEM/F12 per chamber) in Lab-Tek®II Chamber Slides™ (Thermo Fisher). Cells were incubated for 2 days and washed with 400 µL of PBS. After washing, cells were fixed by adding 200 µL 4% paraformaldehyde/PBS to each well for 30 minutes on a rotating platform. The paraformaldehyde solution was then removed and the chambers were detached from the slide, followed by two 5 minute rinses and a 20 minute rinse in PBS.

Cells were incubated in 300 µL of permeabilization/blocking solution (1% bovine serum albumin, 0.3% Triton-X 100 in PBS) at room temperature for 40 minutes.

Permeabilization/blocking solution was removed from the slide and incubated with primary antibody (BMP-2 rabbit polyclonal IgG, Santa Cruz Biotechnology) at a 1:50 dilution in antibody staining solution (0.1% bovine serum albumin, 0.3% Triton-X 100 in PBS) for 2 hours at room temperature and then overnight at 4°C.

Following primary antibody stain, cells were rinsed for 3 times for 5 minutes each in PBS. Cells were then incubated with secondary antibody (Alexa Fluor® 488 goat-anti-rabbit IgG (H+L), Invitrogen) at 1.8 μg per 300 μL of antibody staining solution for 30 min. at room temperature. Following secondary antibody stain, cells were rinsed 3 times for 5 minutes in PBS. Cells were then counterstained using TO-PRO-3-Iodide (Invitrogen) at 1:1000 dilution in PBS for 10 minutes and again rinsed 3 times for 5 minutes in PBS.

Coverslips were mounted on the slides using Fluoromount-G™ mounting medium (SouthernBiotech). Slides were observed on an Olympus FluoView FV1000 confocal laser scanning microscope.

Transfection

HEK293 cells were grown to 85-95% confluency and seeded in a 6-well tissue culture plate (3×10^5 cells per well in 2 mL DMEM/F12). Cells were incubated for 2 days at 37°C and 5% CO_2. Transfection was performed as follows, using Lipofectamine® 2000 (Invitrogen).

For each well of cells, 10 μL of Lipofectamine® 2000 was added to 250 μL of Opti-MEM® I Reduced Serum Media (Gibco), mixed gently and incubated at room temperature for 5 minutes. 4 μg of DNA was added to 250 μL of Opti-MEM and mixture was added to the Lipofectamine® 2000 transfection mixture and mixed gently. Solution was allowed to incubate at room temperature for 20 minutes, after which it was added drop-wise to the well of cells and the

plate was gently rocked to allow mixing. Transfected cells were incubated at 37°C and 5% CO_2 for 2 days before further use to allow for expression of transfected DNA.

Co-Immunoprecipitation

Transfected HEK293 cells were lysed using NP-40 lysis buffer (50 mM Tris-HCl, 150 mM NaCl, 0.5 % NP-40, 50 mM NaF) on ice for 30 minutes. Immediately prior to use, the following were added to the lysis buffer to be at the listed final concentration: 1 mM Na_3VO_4, 1 mM DTT, 1x protease inhibitors (Halt™ Protease Inhibitor Cocktail, Thermo Scientific), 1 mM PMSF. Cells were collected into a microcentrifuge tube and rotated at 4°C for 10 minutes to further lyse cells. After lysis, samples were centrifuged at 14,000 rpm (16,000 rcf) for 5 minutes and supernatant was collected into a new, pre-chilled microcentrifuge tube.

Immunoprecipitation was performed on the lysate samples using either primary antibodies against the tag and Protein A/G PLUS-Agarose beads (Santa Cruz Biotech), or anti-Myc mouse mAb conjugated to sepharose beads (Cell Signaling). For the A/G bead method, lysate was incubated with primary antibody at 1:250 dilution overnight at 4°C. After primary antibody incubation, Protein A/G beads were added for 1 hour at 4°C (5 µL beads per 1 µL primary antibody used). For the sepharose bead method, antibody-conjugated beads were added to cell lysate (20 µL per 500 µL of lysate) and incubated overnight at 4°C.

Following immunoprecipitation, samples were centrifuged at 2000 rpm (326 rcf) for 3 minutes and washed 3 times with cold lysis buffer (500 µL per wash). Samples were then placed in boiling water for 5 minutes and centrifuged for 1 minute to remove protein from beads. Supernatant was saved and stored at 4°C.

MOUSE INFECTION STUDIES

Uninfected Controls

Uninfected wild type and mutant mice were examined to determine if there were any significant innate differences between them without being challenged with bacterial infection. Tissue weights were examined for kidney, liver and spleen. No difference was observed in either kidney or liver size, however mutant spleens were found to be an average of 24% smaller than wild type ($p=0.003$, Table 5, Figure 2).

Because a significant difference between wild type and mutant spleen size was observed in uninfected controls, it was important to determine whether there was some innate structural or functional difference between wild type and mutant spleens. To look at tissue structure, uninfected spleens were sectioned and stained with H&E stain. The spleen has two main structural compartments, red pulp and white pulp, which correspond to its main functions. The red pulp acts as a blood filter to remove pathogens and aging or damaged erythrocytes. As a secondary lymphoid tissue, the spleen also houses many lymphocytes within the white pulp. No obvious differences between wild type and mutant spleens were observed in the H&E stained tissue samples (Figure 3).

In order to test blood filtering function of the spleens, blood cell counts were performed. It would be expected that if the filtering capacity of the mutant spleens was diminished due to their smaller size, then the mutant mice would have higher counts of red blood cells. However,

neither red blood cell, nor white blood cell counts showed any significant difference between uninfected wild type and mutant mice (Figure 4).

As the white pulp is a major site of lymphocyte storage, it was possible that the smaller spleen size observed in the mutant mice was due to fewer lymphocytes being present. To investigate this, the lymphocyte distribution of cells within the spleen was identified using flow cytometry. Common cell markers for many immune cell types were measured (Table 1). There were no differences in the percentage of each cell type present in the wild type and mutant spleens (Figure 5).

Taken together, these results indicate that although the spleens of mutant mice are significantly smaller than wild type prior to any treatment, they appear to still be functional and composed of the same cell types in equal proportions. There were no other significant differences observed between wild type and mutant mice.

Primary Infection

To determine the effect of nBMP2 on the immune response to bacterial infection, nBmp2NLS^{tm} and wild type mice were challenged with a systemic infection of *S. aureus*. An infection dose of 3×10^5 CFU/g was administered intravenously. On the third day after infection, blood, kidney, liver, lymph node and spleen samples showed no difference between wild type and mutant mice in remaining bacterial load (Figure 6). The response to the infection as indicated by percent weight loss (Figure 7) and the percent of mice that survived to day 3 was also the same between wild type and mutants.

Tissue weight was compared for the kidney, liver and spleen samples. While the kidney and liver showed no difference in weight between wild type and mutants, spleens from the

mutant mice were significantly smaller than those from wild type mice (Figure 8). All three tissues had increased in size compared to uninfected controls, however, spleen size increased more than the other two tissue types (Table 5). This is not unexpected, as splenic inflammation is typical in response to infection [13].

Overall, at day 3 after infection, the mutant mice responded to the treatment similarly to wild type, indicating that the primary innate immune response is unaffected by the lack of nuclear BMP2. In order to test the function of the adaptive immune response, which typically takes from 5-7 days to respond, mice were infected and samples were tested 8 days after infection. Since the infection dose of 3×10^5 CFU/g used for the 3 day infections was a fatal dose for approximately 25% of the mice by day 3 (Figure 13a), the dose was lowered to 1×10^4 CFU/g for subsequent experiments.

Both wild type and mutant mice displayed a similar response to the infection as shown by percent weight loss (Figure 9). Both groups appear to begin recovering from the infection around day 5. Post infection bacterial load at day 8 showed no differences between wild type and mutant mice for blood, liver, spleen, kidney and lymph node samples (Figure 10). In both wild type and mutants, bacteria were completely cleared from the blood and only trace amounts remained in liver and spleen. Kidney and lymph nodes samples both had approximately the same amount of bacteria as at day 3.

Wild type and mutant tissue weights were also the same for spleen and kidney samples. Mutant livers were 21% smaller than wild type at day 8 (Table 5). While this difference is statistically significant, there were no differences in liver size prior to infection or at any other stage of infection. Further investigation into the cause of this difference was, therefore, not pursued.

As with the innate response, the adaptive response of the mutant mice to a primary infection appears to function properly. In order to test the ability of the mice to fully recover from the infection, mice were infected and allowed to recover for one month. Samples were tested on day 35 after infection. Both wild type and mutant mice showed complete clearance of bacteria from blood, liver, spleen, kidney and lymph nodes by day 35. In addition, there were no differences in red or white blood cell count (Figure 11). While both wild type and mutant mice tested at day 35 showed equal ability to fully clear the primary infection, mutant mice had a slightly lower percent survival than wild type mice during the first 8 days of infection (Figure 12), indicating that their response may be slightly impaired. However, all other results show that both wild type and mutant mice are able to fully recover from primary infection by day 35.

Secondary Infection

The function of the primary immune response is to clear the infection as quickly as possible. On the other hand, the function of the secondary immune response, executed primarily by B and T lymphocytes, is to prevent the host from succumbing to infection again. Experimental results indicate that, although there are significant differences in some of the main tissues involved, the primary response of mutant mice is fully functional. In order to test the secondary response, mice were challenged with a secondary infection after being allowed to recover from the primary infection. Mice received a lower dose, priming infection at 1×10^4 CFU/g and allowed to recover for 35 days. On day 35, a higher dose secondary infection was administered at 3×10^5 CFU/g.

It was quickly apparent that the ability of the mutant mice to respond to the secondary infection was severely impaired. While nearly all wild type mice survived to day 3 after

secondary infection, only 64% of mutant mice did (Figure 13), even though the response of wild type and mutant mice as shown by percent weight loss showed no difference (Figure 14). This indicates that while wild type mice were effectively immunized by the priming dose prior to secondary infection, mutant mice were not.

Tissue weights again showed no difference in the size of liver or kidney samples, however mutant spleens were 35% smaller than wild type ($p=0.001$, Figure 15). In fact, while the wild type spleens increased in size compared to day 3 after primary infection, mutant spleens were similar in size at day 3 after secondary infection as they were at day 3 after primary infection (Figure 16). This shows a reduced ability of mutant spleens to respond to secondary infection.

With such a severely reduced spleen size, it would be expected that mutant mice would be less efficient at filtering blood and indeed, there was a significant difference in post-infection bacterial load of blood in mutant mice compared to wild type (Figure 17). Mutant mice had a 60 fold increase in the number of bacteria remaining in the blood 3 days after secondary infection compared to wild type (Figure 18). In addition, mutants had lower levels of white blood cells in the blood (Figure 19a). While this difference is not statistically significant, possibly due to the low sample size available, it is suggestive that there could possibly be a difference in the number of circulating lymphocytes. Values for both wild type and mutant samples are clustered together with one outlying sample each, thereby reducing the average difference between them (Figure 19b). A larger sample size would give a more accurate view.

Flow cytometry analysis of the spleen showed no difference between wild type and mutant mice for any of the immune cells tested (Figure 20). However, histological analysis of post-secondary infection spleens showed lower levels of hemosiderin laden macrophages in the

mutants compared to wild type (Figure 21). It is a normal function for macrophages in the spleen to engulf damaged erythrocytes or free hemoglobin in order to recycle and store the iron contained therein. Hemosiderin is an iron storage complex produced by this process. While there is no difference in macrophage abundance in wild type or mutant spleens, as indicated by the flow cytometry data, the lack of hemosiderin laden macrophages within mutant spleens indicates that macrophage phagocytic function is disrupted in the mutant mice.

Along with the differences observed in the spleen, the lymph nodes of wild type and mutant mice also showed significantly different responses to secondary infection. Because corresponding lymph node samples were not able to be obtained from every mouse examined, an accurate quantitative comparison of wild type and mutant lymph node size was not able to be performed. However, it was observed that lymph nodes in wild type mice following secondary infection were consistently larger and easier to locate than in mutant mice. In particular, the lumbar pair of lymph nodes was considerably smaller in mutant mice than wild type (Figure 22). Flow cytometry analysis revealed that there were significantly lower levels of $CD4^+$ and $CD8^+$ T-cells in mutant lymph nodes compared to wild type (Figure 23). Mutant $CD4^+$ T-cell levels were 70% of wild type ($p=0.033$), and mutant $CD8^+$ T-cell levels were 61% of wild type ($p=0.040$).

In addition to the significantly lower levels of $CD4^+$ and $CD8^+$ T-cells observed in mutant lymph nodes, two $CD4^+$ T-cell subsets also showed differences in wild type and mutant levels. CD4+/CD25+ regulatory T-cell levels were 68% higher in mutants ($p=0.064$) and $CD4^+/CD62L^+$ naïve helper T-cells were 45% lower in mutants ($p=0.062$). Also, mutants had much higher levels of $F4/80^+$ mature macrophages present in the lymph nodes than wild type ($p=0.144$). While these differences are not quite statistically significant at the 0.05 level of significance, they

suggest that there is also a possible difference the level of these $CD4^+$ T-cell subsets and mature macrophages present in mutant lymph nodes after secondary infection.

T-cells come from hematopoietic precursor cells formed in the bone marrow and mature within the thymus. While there were lower levels of T-cells found within the lymph nodes of mutant mice, there were no differences between mutant and wild type mice in $CD4^+$ or $CD8^+$ T-cell levels in the thymus (Figure 24). This indicates that T-cell development is functional in mutant mice and the observed deficiencies in lymph node T-cells (Figure 25) are likely due to disruption of function, such as migration signaling pathways, rather than development.

IDENTIFICATION OF NBMP2 BINDING PARTNERS

In order to better understand how nBMP2 functions within the cell, it is important to identify the other proteins it interacts with. This was accomplished using Co-IP from transfected HEK293 cells. In order to be confident that interactions observed were valid, it was necessary to first verify that nBMP2 is expressed endogenously in HEK293 cells. Immunofluorescent staining of non-transfected cells shows endogenous expression of nBMP2 (Figure 26).

Tagged versions of nBmp2 were prepared using site-directed mutagenesis. FLAG, Myc and HA tags were inserted upstream and downstream of the gene so that they would be located at the N- or C-terminus of the expressed protein. Of the six possible variations (N-FLAG, C-FLAG, N-Myc, C-Myc, N-HA, C-HA), five were successfully created. After multiple attempts, transformation of competent cells using N-HA was unsuccessful, so the other five versions were used.

Transfection of HEK293 cells with C-Myc-nBMP2 resulted in successful expression of tagged protein (Figure 27a). Following Co-IP with Myc-conjugated sepharose beads, the tagged

protein was still present in the sample, as expected. Using A/G beads for the Co-IP also yielded purified nBmp2, however a lower amount was present, along with higher levels of non-specific binding of the A/G beads (Figure 27b).

Due to unavailability of the mass spectrometry equipment, samples have not been able to be analyzed at this point. This will be completed by future students.

It has been shown herein that lack of nuclear BMP2 results in an impaired secondary immune response to systemic *S. aureus* infection in mice. Mutant mice do not appear to be innately immunocompromised, in that their response to primary infection is similar to that of wild type mice. In contrast, mutant response to secondary infection is limited. Wild type mice showed an increased rate of survival after secondary infection than after primary infection, indicating that they were effectively immunized by primary exposure to the pathogen. Mutant mice, on the other hand, showed no effect of immunization and actually had a decreased rate of survival following secondary infection compared to primary infection. These results indicate dysfunction of the secondary immune response in the mutant mice, particularly in memory cells which provide the protective effect against repeated exposure to a pathogen.

Previous work with nBmp2NLS^{tm} mutant mice has shown that they have impaired intracellular calcium transport, resulting in decreased muscle strength and cognitive disorders. Intracellular calcium transport is a key component of immune cell activation and migration signaling pathways [9-12, 14], particularly in B- and T-lymphocytes. Therefore, it is likely that the observed immune response in the mutant mice is due, at least in part, to reduced B-and T-cell function caused by disrupted intracellular calcium transport.

The reduced levels of T-cells within lymph nodes of nBmp2NLS^{tm} mutant mice following secondary infection further support the hypothesis that lack of nBMP2 impairs lymphocyte function. T-cells are generated in the bone marrow and mature in the thymus. Following maturation, they are released into circulation throughout the body. In response to infection, it is common for lymph nodes to enlarge due to accumulation and proliferation of T-

cells as they respond to activation signals from antigen presenting cells. Similar levels of T-cells were observed in the thymus of both mutant and wild type mice, indicating that T-cell generation is not affected in the mutants. Within the lymph nodes, however, significantly lower levels of both $CD4^+$ and $CD8^+$ T-cells were present in mutant mice than in wild type mice. Therefore, it is possible that, although T-cell generation is unaffected in mutant mice, the ability of those T-cells to respond to activation and migratory signals has been disrupted.

In order to further determine the effect of nBMP2 on lymphocyte function, it will be important to test antibody production in mutant mice. Proper antibody production by B-cells is a key factor in secondary immune response. B-cells and T-cells are both direct descendants of small lymphocyte precursor cells and are similar in many ways; including surface morphology [15] and dependence on intracellular calcium transport for proper activation signaling [12, 16, 17]. I suspect that, in addition to inhibiting T-cell function, lack of nBMP2 also impairs B-cell function. Furthermore, as $CD4^+$ helper T-cells are a main source of antigen presentation to B-cells, leading to their activation and subsequent antibody production, a deficiency in T-cell function could easily lead to decreased antibody production.

In addition to the T-cell phenotypes observed in mutant mice, macrophage function was also inhibited. Following secondary infection, mutant spleens showed much lower levels of hemosiderin laden macrophages. Hemosiderin is an iron storage complex produced when macrophages engulf damaged erythrocytes or free hemoglobin in order to recycle and store the iron contained therein [13]. While this process is typically the result of hemorrhage, it is possible that it is the result of *S. aureus* infection. Iron is an essential nutrient for both *S. aureus* and the hosts it infects. One mechanism of pathogenesis employed by *S. aureus* is the secretion of hemolysins in order to rupture red blood cells and gain access to the iron stored within

hemoglobin [18, 19]. This would give splenic macrophages the opportunity to engulf high levels of free hemoglobin resulting from red blood cell lysis. The high level of hemosiderin laden macrophages observed in wild type spleens, but not in mutants, provides evidence that lack of nuclear BMP2 leads to decreased phagocytic function of macrophages.

Neutrophils, one of the most common white blood cell types and efficient phagocytes, are closely related to macrophages as both are descendants of myeloblasts. Neutrophils are key players in the immune response to *S. aureus* infection [20, 21]. Berger *et al*. [22] have shown that intracellular calcium concentration regulation is necessary for increased complement receptor expression involved in neutrophil activation. In addition, intracellular calcium transport is a key element of neutrophil chemotaxis [23] and phagocytosis [24]. Although neutrophils are primarily involved in innate immune function, which appears to be functional in nBmp2NLS^{tm} mutant mice, Rakhmilevich [25] has shown that neutrophil function is necessary for resolution of both primary and secondary infection with *Listeria monocytogenes*. It is, therefore, also possible that neutrophil function has been disrupted in nBmp2NLS^{tm} mutant mice, leading to poor response to secondary infection.

Along with impaired function of immune cells, lack of nBMP2 in mice also leads to reduced spleen size relative to wild type mice. This difference was present prior to treatment and throughout various stages of infection, however, it was most pronounced following secondary infection. While wild type spleens continued to increase in size following secondary infection, mutant spleens did not, indicating a disruption of splenic function. Teixeira *et al.* [26] have shown that the spleen is necessary for proper recovery from *S. aureus* infection. Accordingly, nBmp2NLS^{tm} mutant mice showed reduced spleen function, as well as a severely impaired immune response to secondary infection with *S. aureus*.

The importance of proper spleen function has been well established and the effects of hyposplenism and asplenism on the immune response have been thoroughly studied [27-31]. Absence of the spleen or loss of splenic function leaves individuals at a much higher risk of rapid onset of septicemia and overwhelming infection [32]. Much of the murine research related to spleen function involves partial or complete splenectomy as a method of determining the effects of the spleen on immune function. Currently, there is not a mouse model available for use in studying the effect of reduced spleen size on immune response. The nBmp2NLS^{tm} mouse line has potential to be used as such a model, thereby allowing research of spleen function without the need for surgical procedures.

In order to more fully understand the involvement of nBMP2 in the immune response to bacterial infection, it will be vital to determine which pathways it is involved in and the molecular mechanisms thereof. Work is currently underway to identify binding partners of nBMP2 using co-immunoprecipitation and mass spectrometry. This will provide important clues for determining, on a molecular level, how nBMP2 affects the immune response.

Table 1: Antibodies used for lymphocyte identification.

	Marker	Stain	Antibody	Clone	eBioscience Reference Number
Group 1	CD11b	FITC	Anti-Mouse CD11b FITC	M1/70	11-0112-82
	CD8a	PE	Anti-Mouse CD8a PE	53-6.7	12-0081-82
	CD4	APC	Anti-Mouse CD4 eFluor® 660	GK1.5	50-0041-82
	Gr-1	PE-Cy7	Anti-Mouse Ly-6g (Gr-1) PE-Cy7	RB6-8C5	25-5931-82
Group 2	B220	FITC	Anti-Human/Mouse CD45R (B220) FITC	RA3-6B2	11-0452-82
	CD8a	PE	Anti-Mouse CD8a PE	53-6.7	12-0081-82
	CD4	APC	Anti-Mouse CD4 eFluor® 660	GK1.5	50-0041-82
	Gr-1	PE-Cy7	Anti-Mouse Ly-6g (Gr-1) PE-Cy7	RB6-8C5	25-5931-82
Group 3	CD11c	FITC	Anti-Mouse CD11c FITC	N418	11-0114-82
	CD5	PE	Anti-Mouse CD5 PE	53-7.3	12-0051-82
	CD4	APC	Anti-Mouse CD4 eFluor® 660	GK1.5	50-0041-82
	Gr-1	PE-Cy7	Anti-Mouse Ly-6g (Gr-1) PE-Cy7	RB6-8C5	25-5931-82
Group 4	F4/80	FITC	Anti-Mouse F4/80 FITC	BM8	11-4801-82
	CD3e	PE	Anti-Mouse CD3e PE	145-2C11	12-0031-82
	CD4	APC	Anti-Mouse CD4 eFluor® 660	GK1.5	50-0041-82
	Gr-1	PE-Cy7	Anti-Mouse Ly-6g (Gr-1) PE-Cy7	RB6-8C5	25-5931-82
Group 5	CD4	FITC	Anti-Mouse CD4 FITC	GK1.5	11-0041-82
	CD44	PE	Anti-Human/Mouse CD44 PE	IM7	12-0441-82
	CD25	APC	Anti-Mouse CD25 APC	PC61.5	17-0251-82
	Gr-1	PE-Cy7	Anti-Mouse Ly-6g (Gr-1) PE-Cy7	RB6-8C5	25-5931-82
	CD62L	APC-Cy7	Anti-Mouse CD62L APC-eFluor® 780	MEL-14	47-0621-82

Table 2: Tissue processor Program A.

Stage	Reagent	Time (h)
1	70% EtOH	1
2	80% EtOH	1
3	80% EtOH	1
4	95% EtOH	1
5	95% EtOH	1
6	100% EtOH	1
7	100% EtOH	2
8	Xylene	1
9	Xylene	1
10	Xylene	1
11	Paraffin	1
12	Paraffin	2.5

Table 3: H&E staining procedure.

Step	Reagent	Time (min:sec)
1	Clear-Rite (Thermo Scientific)	3:00
2	Clear-Rite (Thermo Scientific)	3:00
3	Clear-Rite (Thermo Scientific)	3:00
4	100% EtOH	1:00
5	100% EtOH	1:00
6	95% EtOH	1:00
7	Distilled Water	1:00
8	Hematoxylin 7211 (Thermo Scientific)	1:30
9	Distilled Water	1:00
10	Clarifier (Thermo Scientific)	0:50
11	Distilled Water	1:00
12	Bluing Reagent (Thermo Scientific)	1:00
13	Distilled Water	1:00
14	95% EtOH	0:30
15	Eosin-Y (Thermo Scientific)	1:30
16	100% EtOH	1:00
17	100% EtOH	1:00
18	Clear-Rite (Thermo Scientific)	1:00
19	Clear-Rite (Thermo Scientific)	1:00
20	Clear-Rite (Thermo Scientific)	1:00

Table 4: Primers used for site-directed mutagenesis.

Tag	Primer	Sequence
FLAG	Upstream	Fwd. CCCTTAAAAAGCTGCTCAGCATGGACTACAAGGACGACGACGACAAGGGTGGCGGAGGTGGCTTTGGCCTGAAGCAGAGACC
		Rev. GGTCTCTGCTTCAGGCCAAAGCCACCTCCGCCACCCTTGTCGTCGTCGTCCTTGTAGTCCATGCTGAGCAGCTTTTTAAGGG
	Downstream	Fwd. TGGAGGGTTGCGGGTGTCGCGGTGGCGGAGGTGGCGACTACAAGGACGACGACGACAAGTAGCACAGCAAGATCTAGGATCC
		Rev. GGATCCTAGATCTTGCTGTGCTACTTGTCGTCGTCGTCCTTGTAGTCGCCACCTCCGCCACCGCGACACCCGCAACCCTCCA
Myc	Upstream	Fwd. CCCTTAAAAAGCTGCTCAGCATGGAGCAGAAGCTGATCAGCGAGGAGGACCTGGGTGGCGGAGGTGGCTTTGGCCTGAAGCAGAGACC
		Rev. GGTCTCTGCTTCAGGCCAAAGCCACCTCCGCCACCCAGGTCCTCCTCGCTGATCAGCTTCTGCTCCATGCTGAGCAGCTTTTTAAGGG
	Downstream	Fwd. TGGAGGGTTGCGGGTGTCGCGGTGGCGGAGGTGGCGAGCAGAAGCTGATCAGCGAGGAGGACCTGTAGCACAGCAAGATCTAGGATCC
		Rev. GGATCCTAGATCTTGCTGTGCTACAGGTCCTCCTCGCTGATCAGCTTCTGCTCGCCACCTCCGCCACCGCGACACCCGCAACCCTCCA
HA	Upstream	Fwd. CCCTTAAAAAGCTGCTCAGCATGTACCCTTACGACGTGCCTGACTACGCCGGTGGCGGAGGTGGCTTTGGCCTGAAGCAGAGACC
		Rev. GGTCTCTGCTTCAGGCCAAAGCCACCTCCGCCACCGGCGTAGTCAGGCACGTCGTAAGGGTACATGCTGAGCAGCTTTTTAAGGG
	Downstream	Fwd. TGGAGGGTTGCGGGTGTCGCGGTGGCGGAGGTGGCTACCCTTACGACGTGCCTGACTACGCCTAGCACAGCAAGATCTAGGATCC
		Rev. GGATCCTAGATCTTGCTGTGCTAGGCGTAGTCAGGCACGTCGTAAGGGTAGCCACCTCCGCCACCGCGACACCCGCAACCCTCCA

Start Codon Tag Sequence Glycine Linker Stop Codon

Table 5: Tissue weights.

Liver					
	Day 0	Day 3	Day 8	Day 35	Day 38
Mutant Avg. Weight (g)	1.32	1.41	1.11	1.32	1.32
WT Avg. Weight (g)	1.33	1.47	1.41	1.42	1.46
Difference (Mutant-WT)	-0.01	-0.05	-0.30	-0.10	-0.15
Percent Change (Mutant/WT)	-0.5%	-3.7%	-21.2%	-6.9%	-10.0%
P value	0.946	0.522	0.001	0.634	0.328
Mutant Standard Deviation	0.205	0.179	0.033	0.214	0.151
WT Standard Deviation	0.265	0.229	0.070	0.062	0.301
Mutant Sample Size	12	12	3	2	5
WT Sample Size	12	12	4	3	6

Spleen					
	Day 0	Day 3	Day 8	Day 35	Day 38
Mutant Avg. Weight (g)	0.08	0.14	0.15	0.17	0.16
WT Avg. Weight (g)	0.11	0.17	0.18	0.10	0.25
Difference (Mutant-WT)	-0.03	-0.04	-0.03	0.06	-0.09
Percent Change (Mutant/WT)	-23.8%	-21.8%	-15.0%	63.2%	-35.4%
P value	0.003	0.018	0.659	0.582	< 0.001
Mutant Standard Deviation	0.018	0.027	0.060	0.119	0.029
WT Standard Deviation	0.029	0.043	0.093	0.017	0.063
Mutant Sample Size	20	12	3	2	11
WT Sample Size	20	12	4	3	12

Kidney					
	Day 0	Day 3	Day 8	Day 35	Day 38
Mutant Avg. Weight (g)	0.43	0.49	0.40	0.28	0.35
WT Avg. Weight (g)	0.38	0.47	0.40	0.31	0.38
Difference (Mutant-WT)	0.05	0.02	0.00	-0.03	-0.03
Percent Change (Mutant/WT)	13.3%	4.9%	0.6%	-10.9%	-7.5%
P value	0.061	0.540	0.971	0.646	0.456
Mutant Standard Deviation	0.069	0.105	0.092	0.077	0.053
WT Standard Deviation	0.057	0.075	0.052	0.032	0.068
Mutant Sample Size	12	12	3	2	5
WT Sample Size	12	12	4	3	6

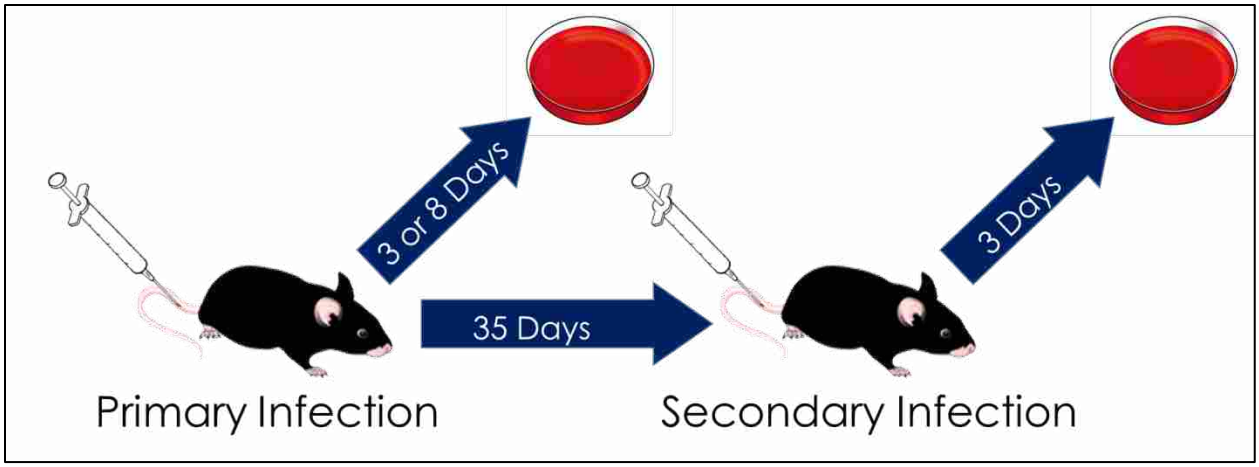

Figure 1: Experimental setup diagram for primary and secondary infections.

For primary infection, mice were infected via tail vein injection with a dose of either 3×10^5 CFU/g or 1×10^4 CFU/g and samples were tested either 3 or 8 days, respectively, after infection (indicated by agar plate). For secondary infections, mice received a priming dose of 1×10^4 CFU/g, were allowed to recover for 35 days, and then received a secondary infection of 3×10^5 CFU/g via tail vein injection. Samples were tested 3 days after secondary infection.

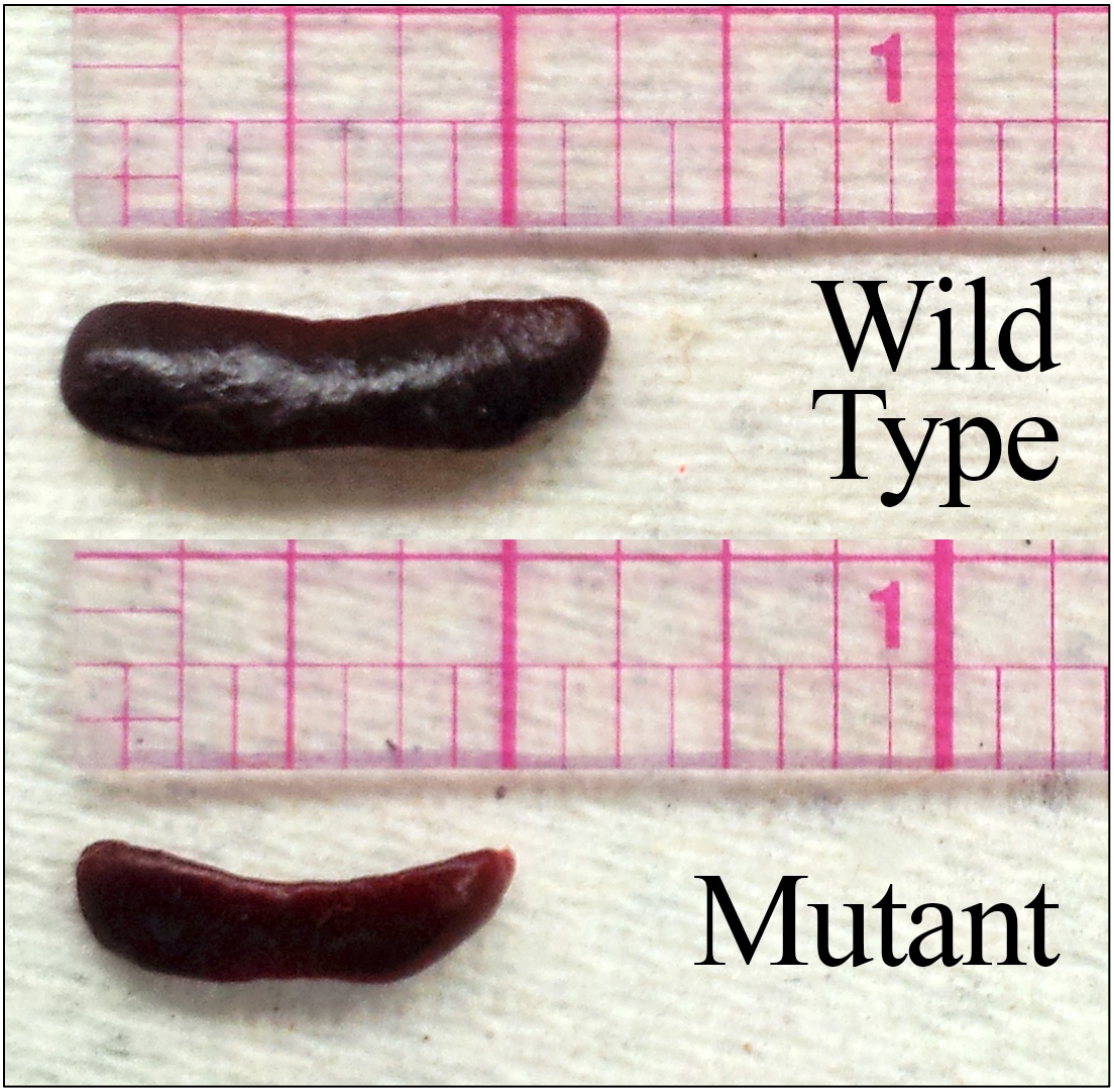

Figure 2: Uninfected spleen size comparison.

Representative samples of uninfected mutant and wild type spleens from 6 month old mice are shown. Ruler mark is equal to 1 inch. nBMP2NLS^{tm} mutant spleen size is reduced compared to wild type.

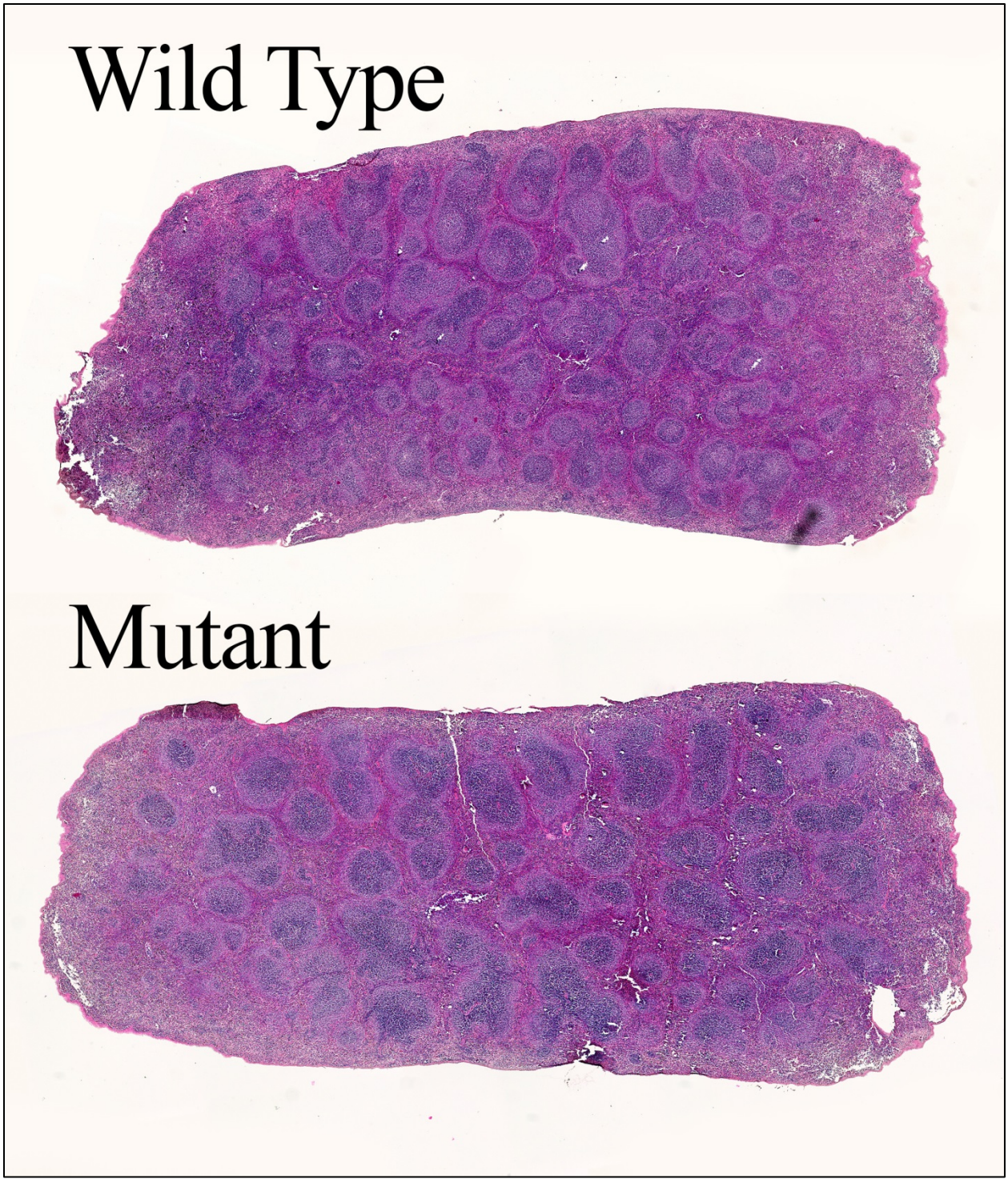

Figure 3: Histology of wild type and mutant spleens.

Paraffin embedded spleen sections from uninfected, 6 month old mice were stained with hematoxylin and eosin (H&E). Both wild type and mutant spleens show similar gross anatomy and white pulp to red pulp ratios.

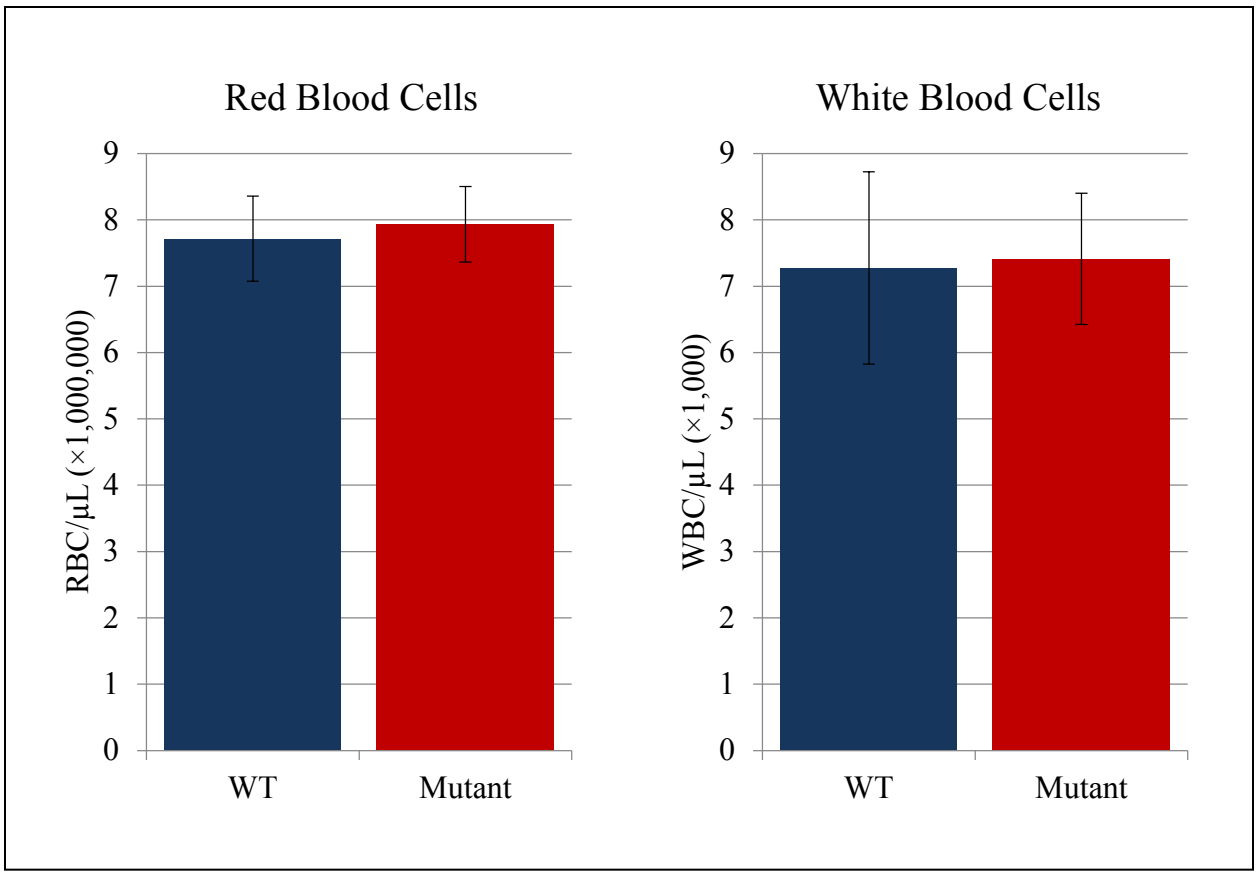

Figure 4: Blood cell counts of uninfected mice.

Red blood cell and white blood cell counts for uninfected mice show no difference between wild type and mutants. Error bars indicate standard error. RBC: n_{wt}=11 n_{mut}=13. WBC: n_{wt}=8 n_{mut}=10.

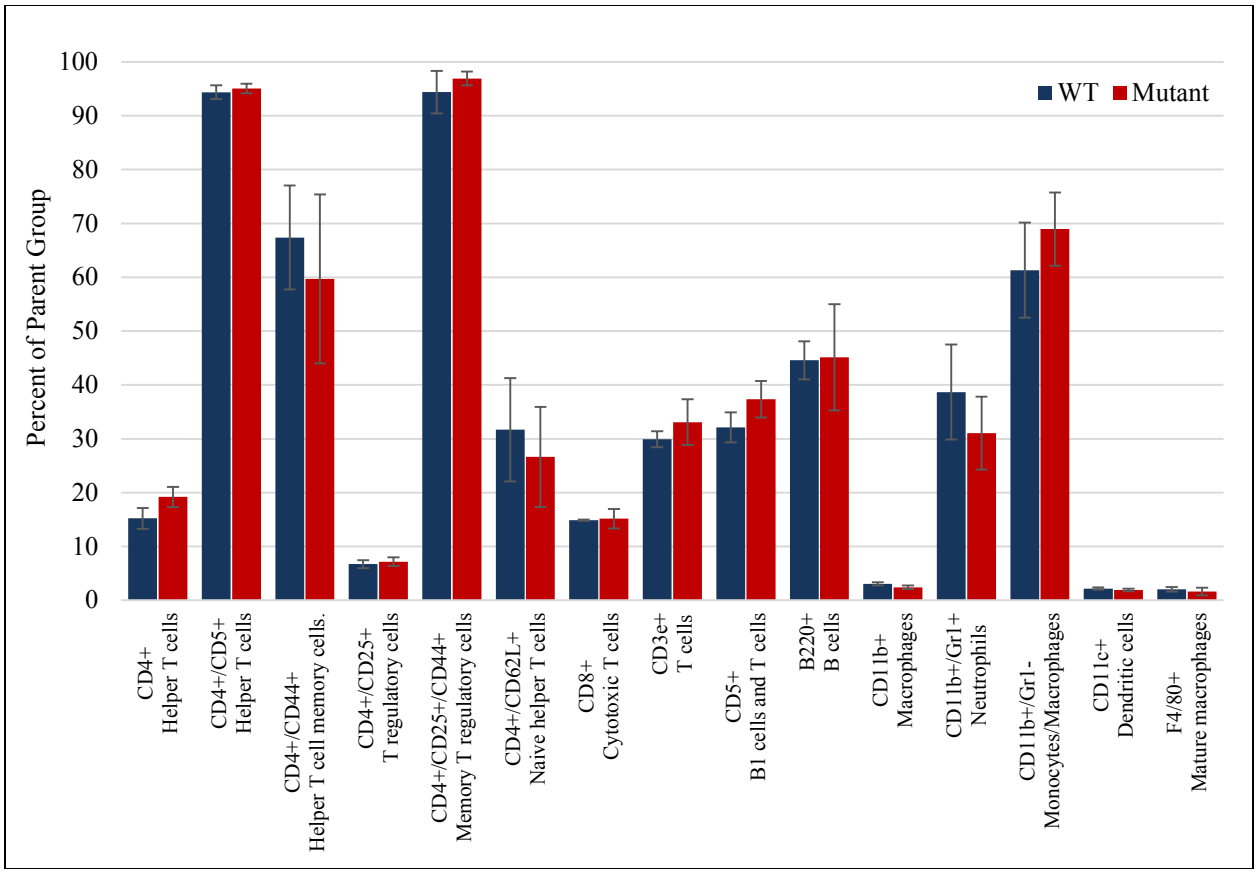

Figure 5: Lymphocyte populations in uninfected spleens.

Spleen cell types were measured using flow cytometry. No significant differences were observed between mutant and wild type for any of the cell types tested. Error bars indicate standard error. $n_{wt}=3$ $n_{mut}=3$. Values shown are percent of parent group. For example, CD4+ value is the percent of lymphocytes that are CD4+. CD4+/CD5+ value is the percent of CD4+ lymphocytes that are also CD5+.

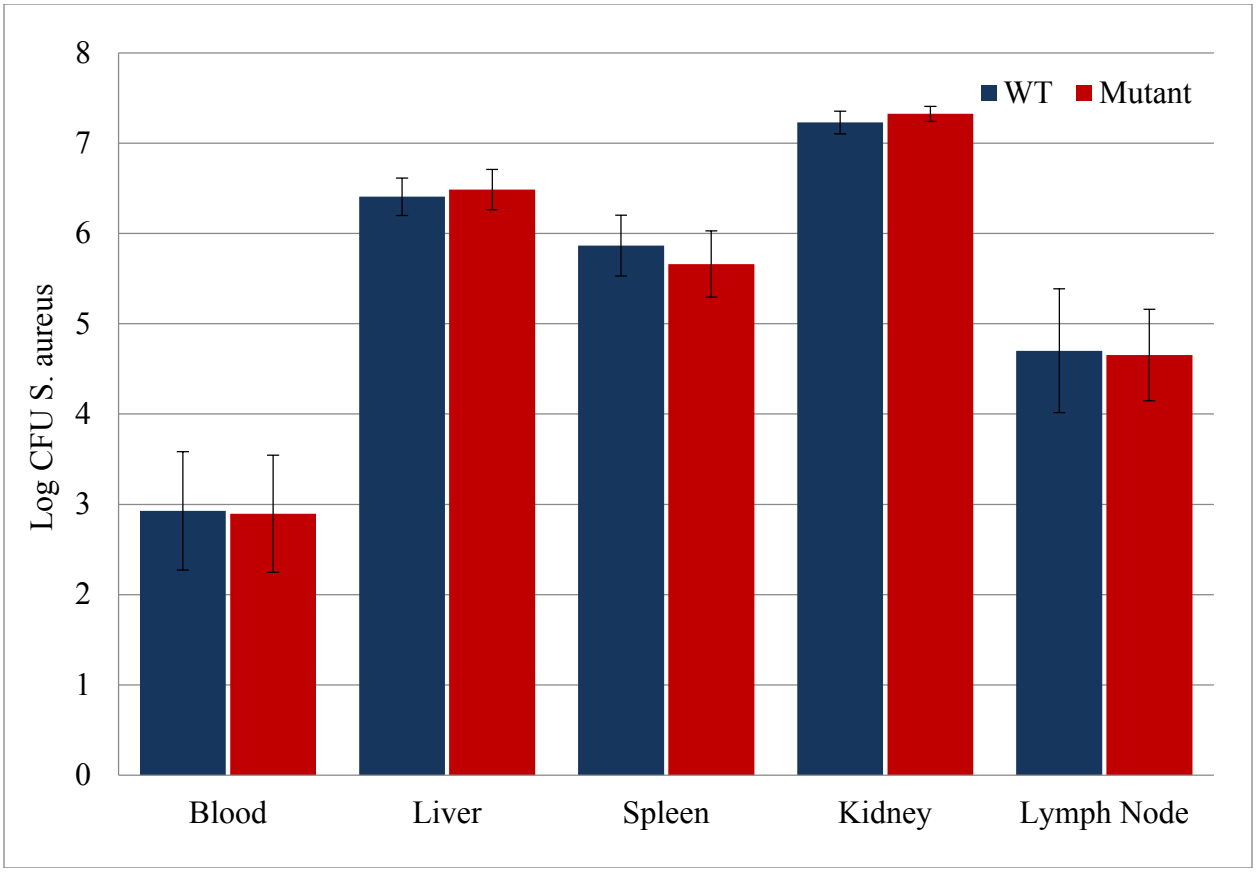

Figure 6: Bacterial load on day 3 after primary infection.

Tissue samples tested 3 days after primary infection show no difference in bacterial load between wild type and mutant mice. Results shown are CFU/mL for blood samples and CFU/g for liver, spleen, kidney and lymph node samples. Error bars indicate standard error. $n_{wt}=12$ $n_{mut}=12$.

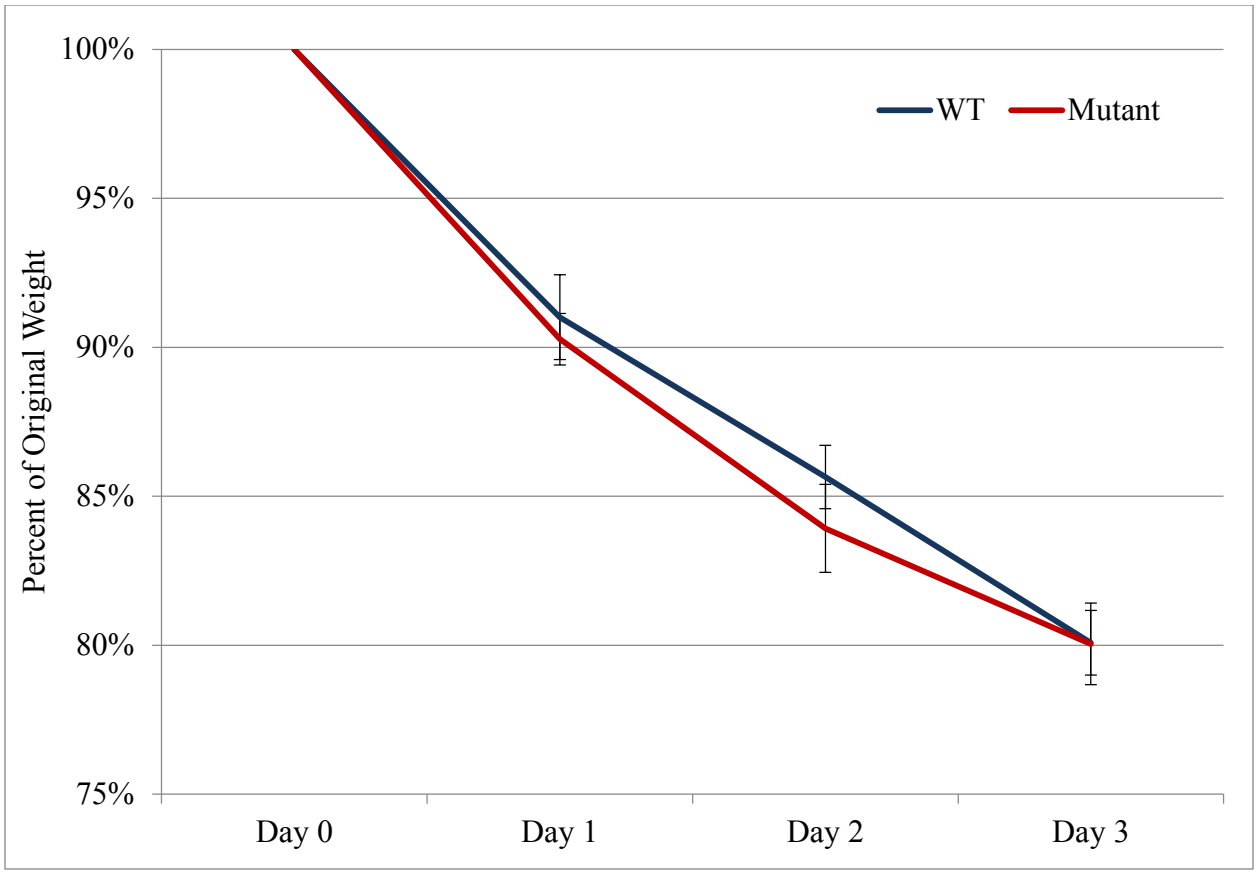

Figure 7: Primary infection weight loss.

Wild type and mutant mice showed no difference in percent weight loss following primary infection. Error bars indicate standard error. n_{wt}=12 n_{mut}=12.

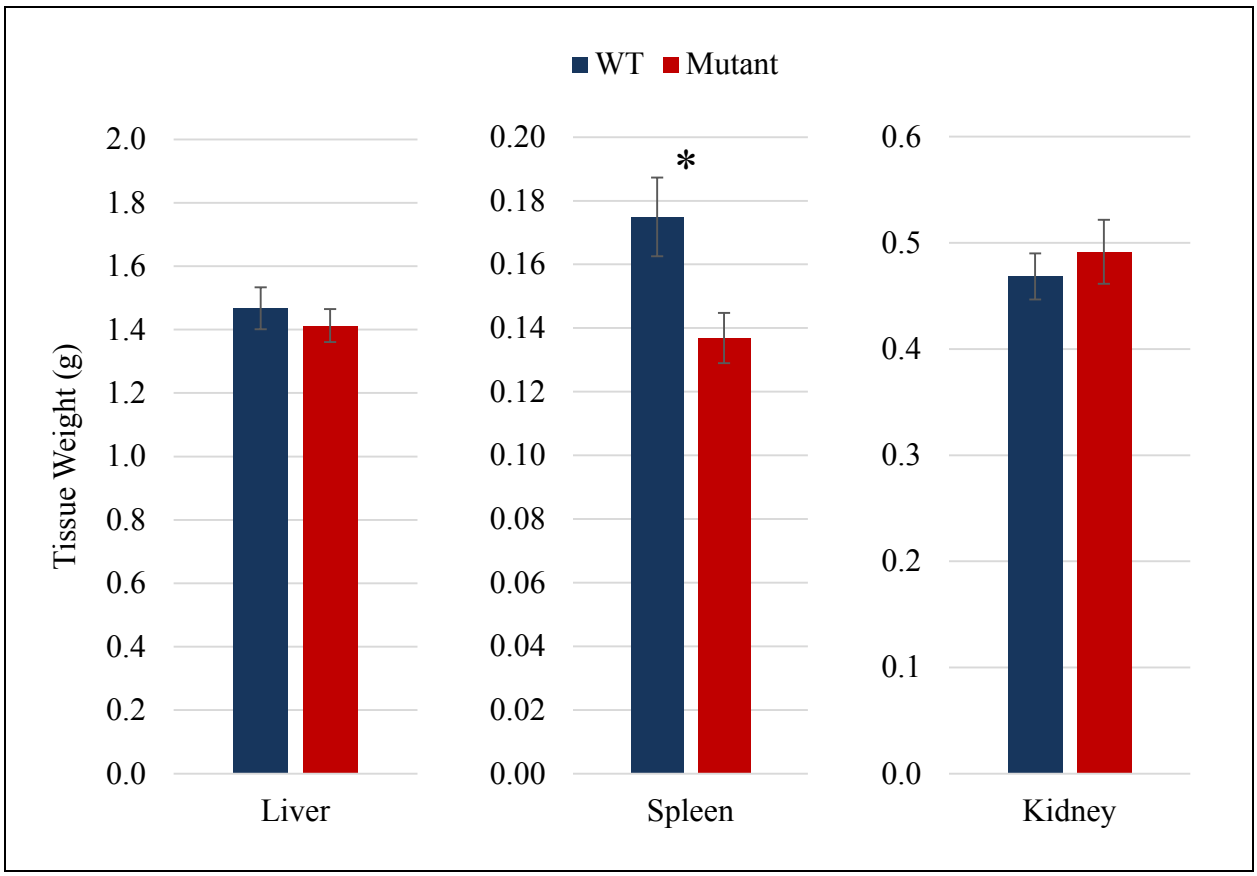

Figure 8: Tissue weights 3 days after primary infection.

Tissue weights were measured on day 3 after primary infection. Mutant and wild type mice showed no significant difference in liver or kidney weight. Mutant spleens were 22% smaller than wild type (p=0.018). Error bars indicate standard error. n_{wt}=12 n_{mut}=12.

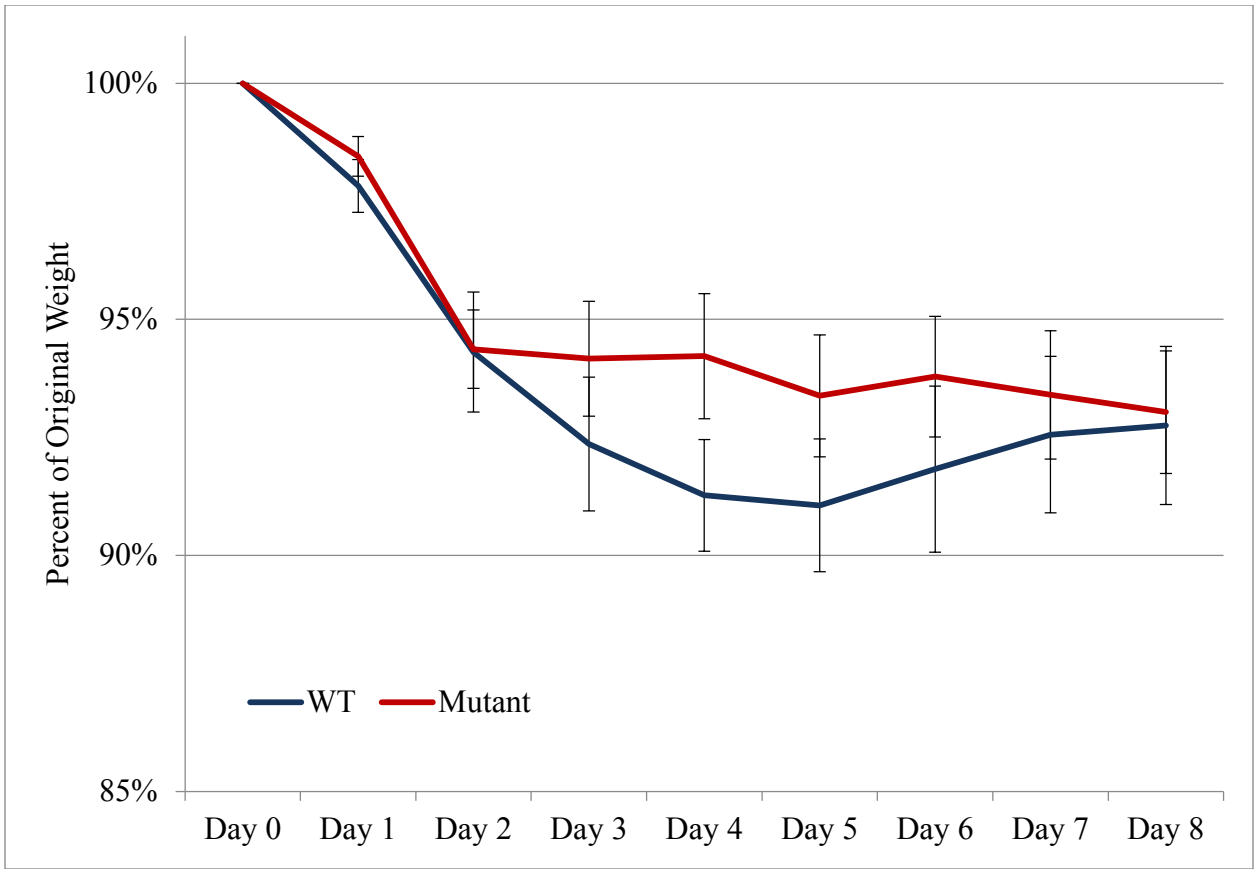

Figure 9: Percent weight loss 8 days after primary infection.

Wild type and mutant mice showed no difference in percent weight loss 8 days after primary infection. Results shown include data from first 8 days after infection for mice examined on day 8 after primary infection, day 35 after primary infection and mice from secondary infection group. Error bars indicate standard error. n_{wt}=19 n_{mut}=19.

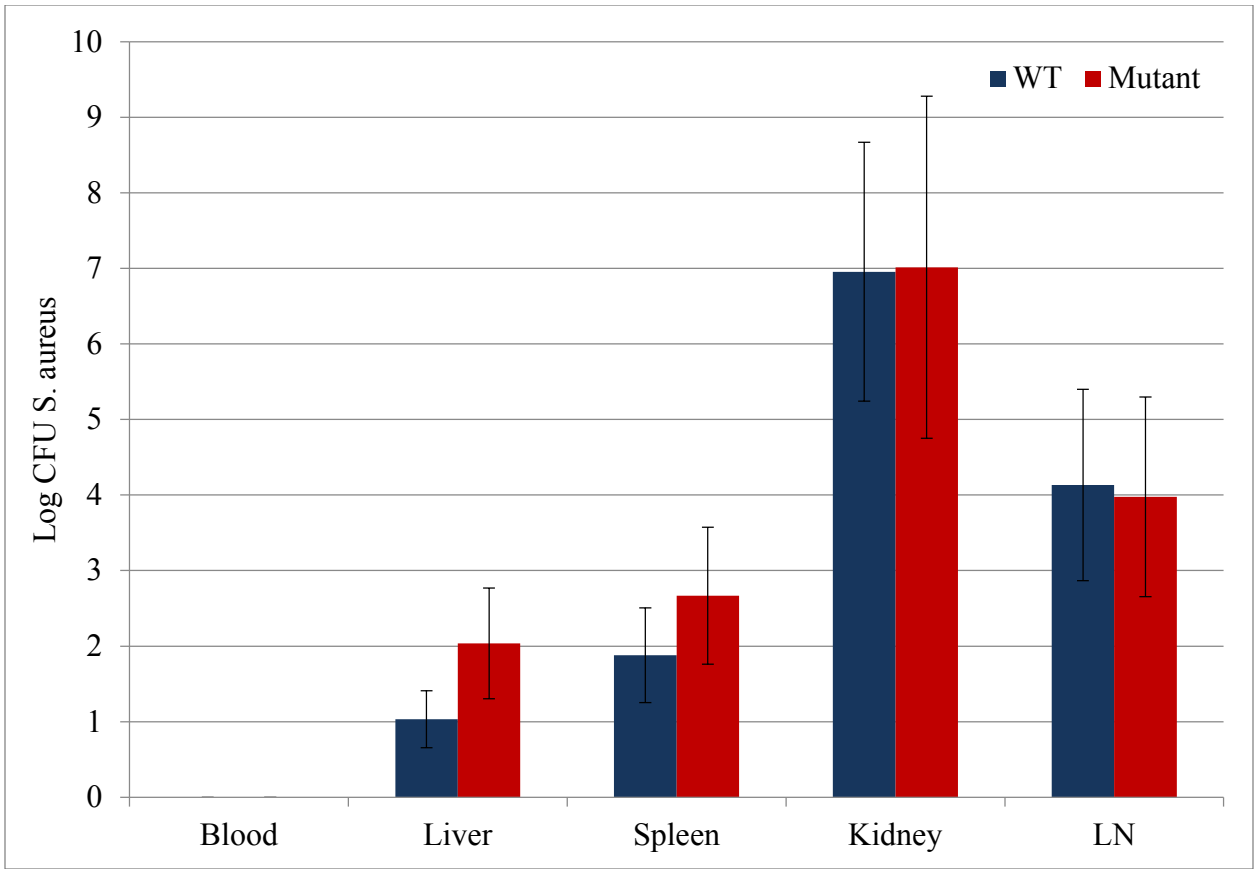

Figure 10: Bacterial load on day 8 after primary infection.

Tissue samples tested 8 days after primary infection show no significant difference in bacterial load between wild type and mutant mice for any tissues tested. In both genotypes, bacteria was completely cleared from blood and reduced in liver and spleen, compared to 3 days after primary infection. Results shown are CFU/mL for blood samples and CFU/g for liver, spleen, kidney and lymph node samples. Error bars indicate standard error. $n_{wt}=4$. $n_{mut}=3$.

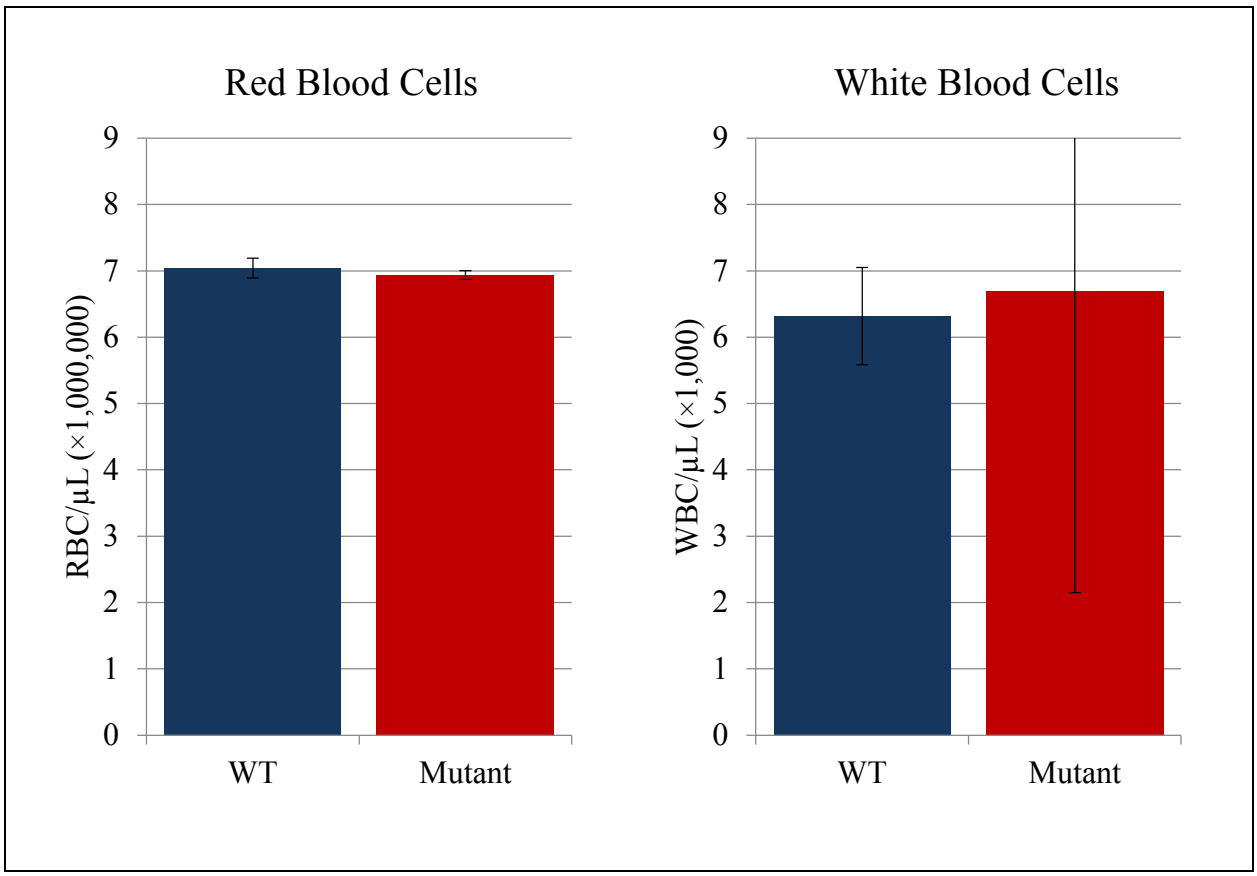

Figure 11: Day 35 blood cell counts.

Mice were allowed to recover for 35 days after primary infection. Red blood cell and white blood cell counts show no difference between wild type and mutants. Error bars indicate standard error. $n_{wt}=3$. $n_{mut}=2$.

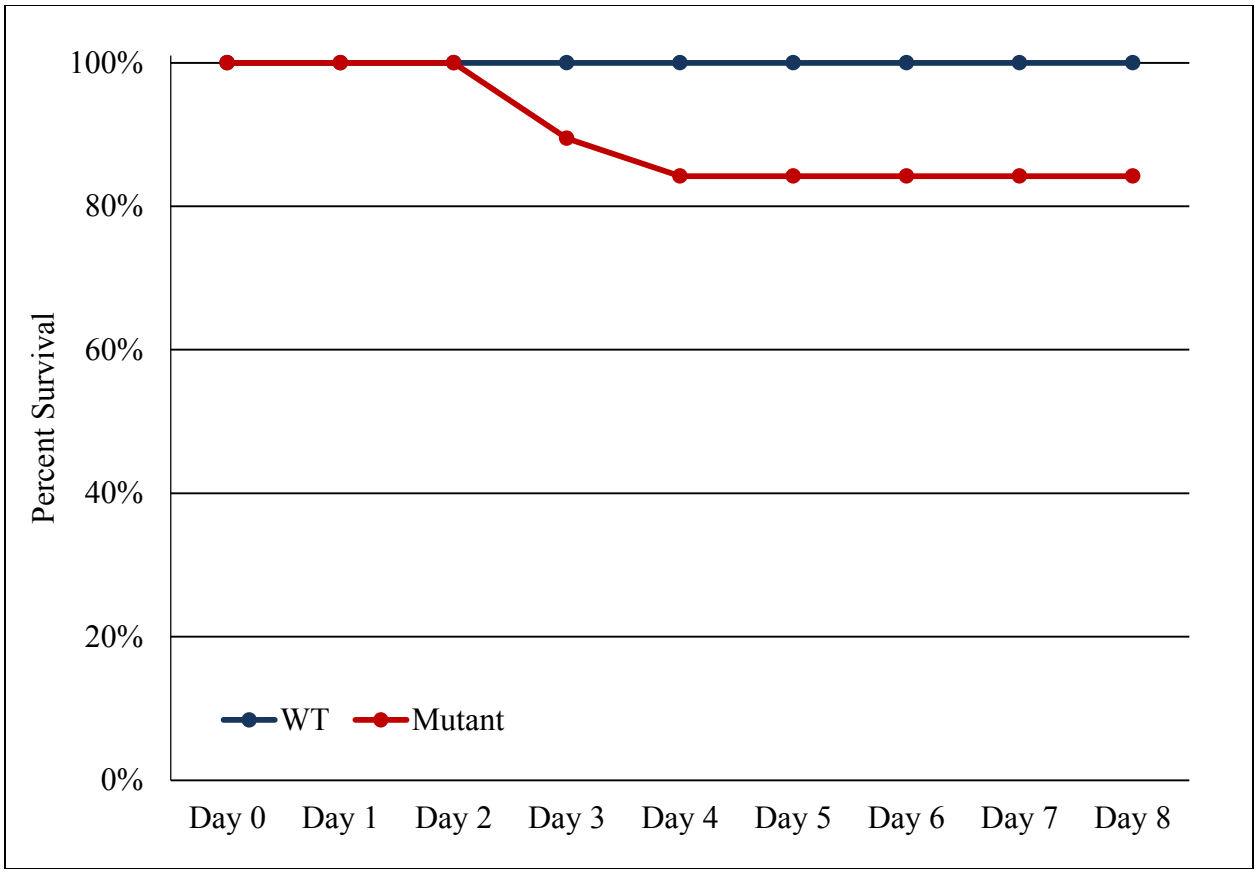

Figure 12: Percent survival 8 days after primary infection.

Mice were infected with 1×10^4 CFU/g and percent survival was measured. Mutant mice showed slightly lower survival to day 8 after primary infection, compared to wild type mice. Results shown include data from first 8 days after infection for mice examined on day 8 after primary infection, day 35 after primary infection and mice from secondary infection group. $n_{wt}=19$ $n_{mut}=19$.

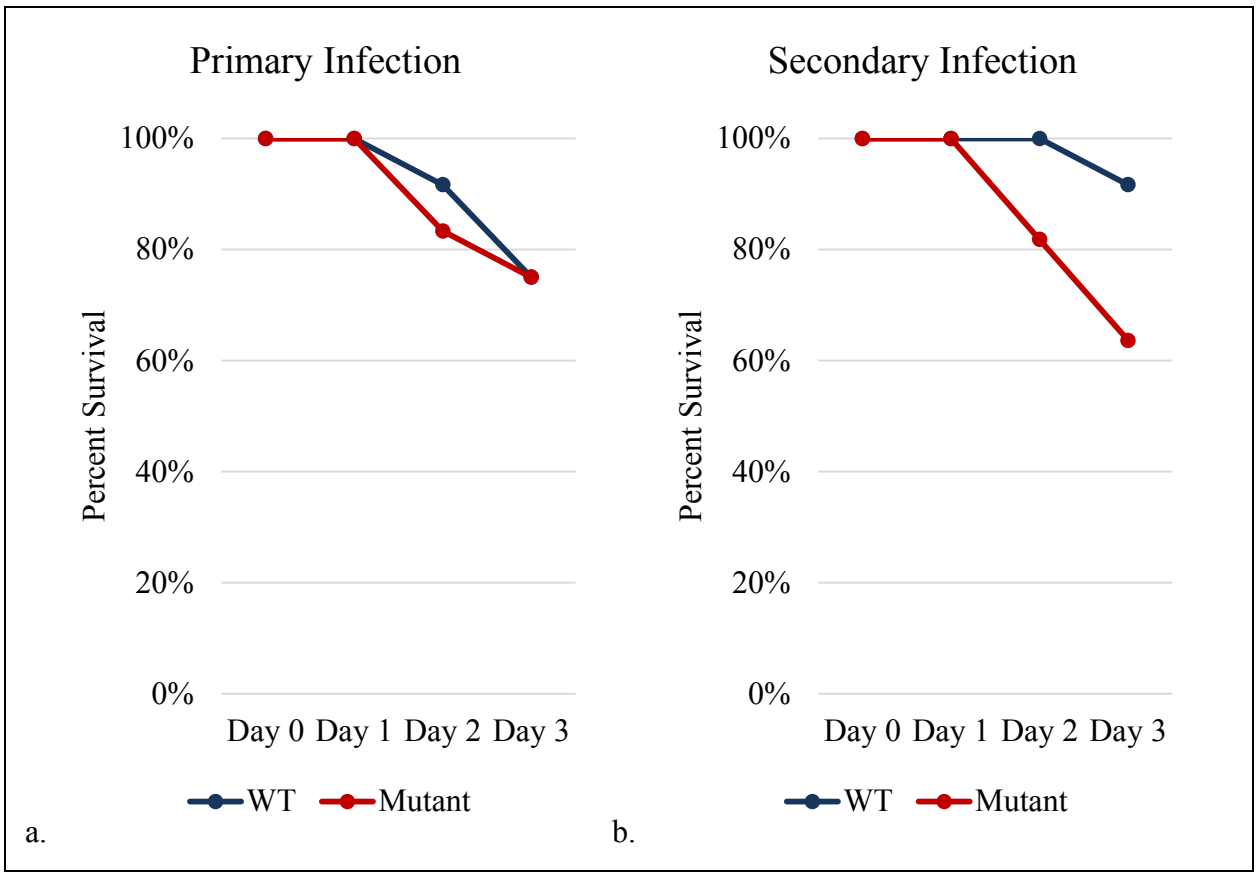

Figure 13: Percent survival after primary and secondary infections.

Survival rates following primary and secondary infections were measured. For primary infections, mice received a dose of 3×10^5 CFU/g. For secondary infections, mice received a priming dose of 1×10^4 CFU/g, followed by a secondary infection of 3×10^5 CFU/g 35 days later. (a.) Mutant and wild type mice showed similar survival rates following primary infection. $n_{wt}=12$ $n_{mut}=12$. (b.) Mutant mice had a lower rate of survival to day 3 after secondary infection compared to wild type. $n_{wt}=12$ $n_{mut}=11$. Wild type mice have an increased rate of survival after secondary infection, compared to primary infection, indicating that they were properly immunized by the priming dose. Mutant mice, however, actually have a lower rate of survival after secondary infection than after primary infection, indicating that they were not properly immunized and the secondary immune response is impaired in mutant mice.

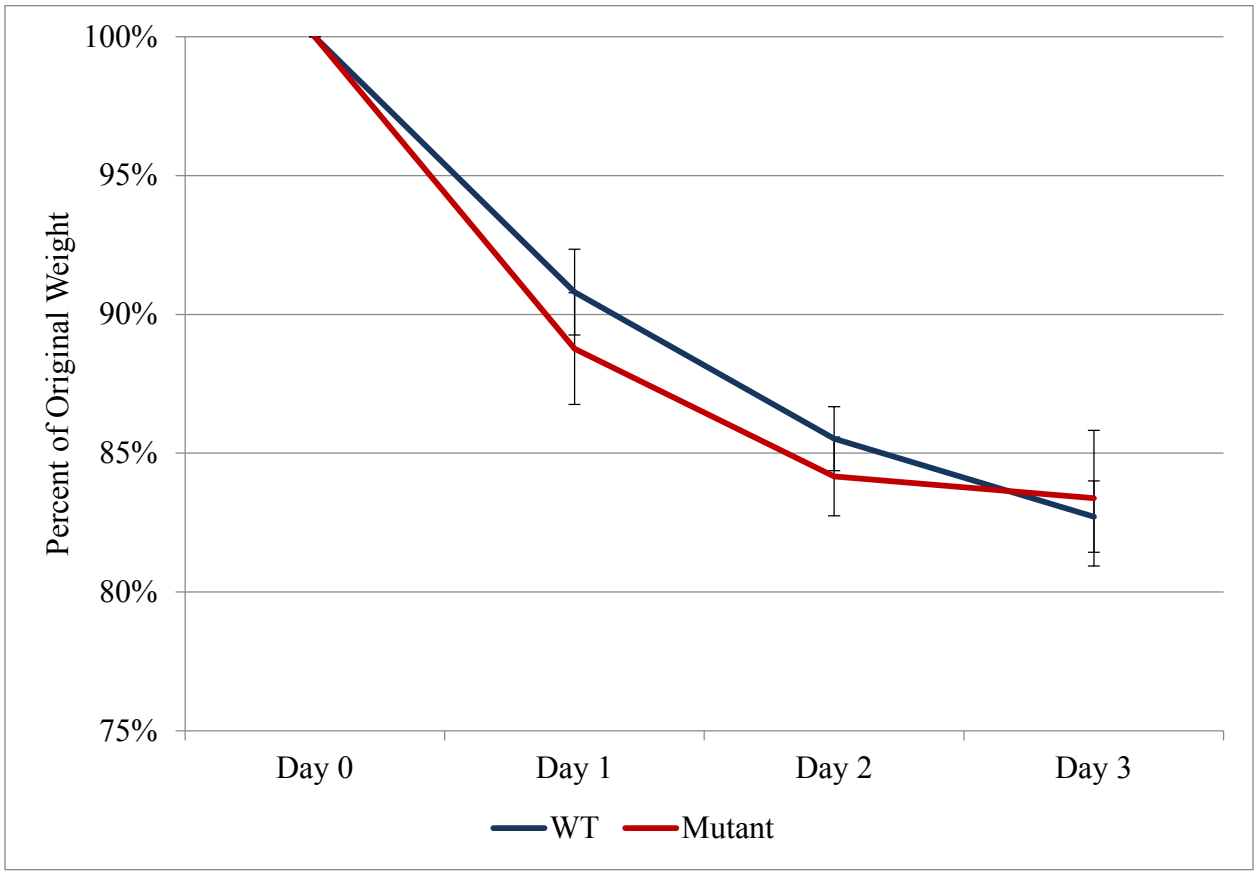

Figure 14: Percent weight loss after secondary infection.

Wild type and mutant mice showed no difference in percent weight loss following secondary infection. Results shown include data from mice used for secondary infection bacterial load tests as well as flow cytometry analysis. Error bars indicate standard error. $n_{wt}=12$ $n_{mut}=11$

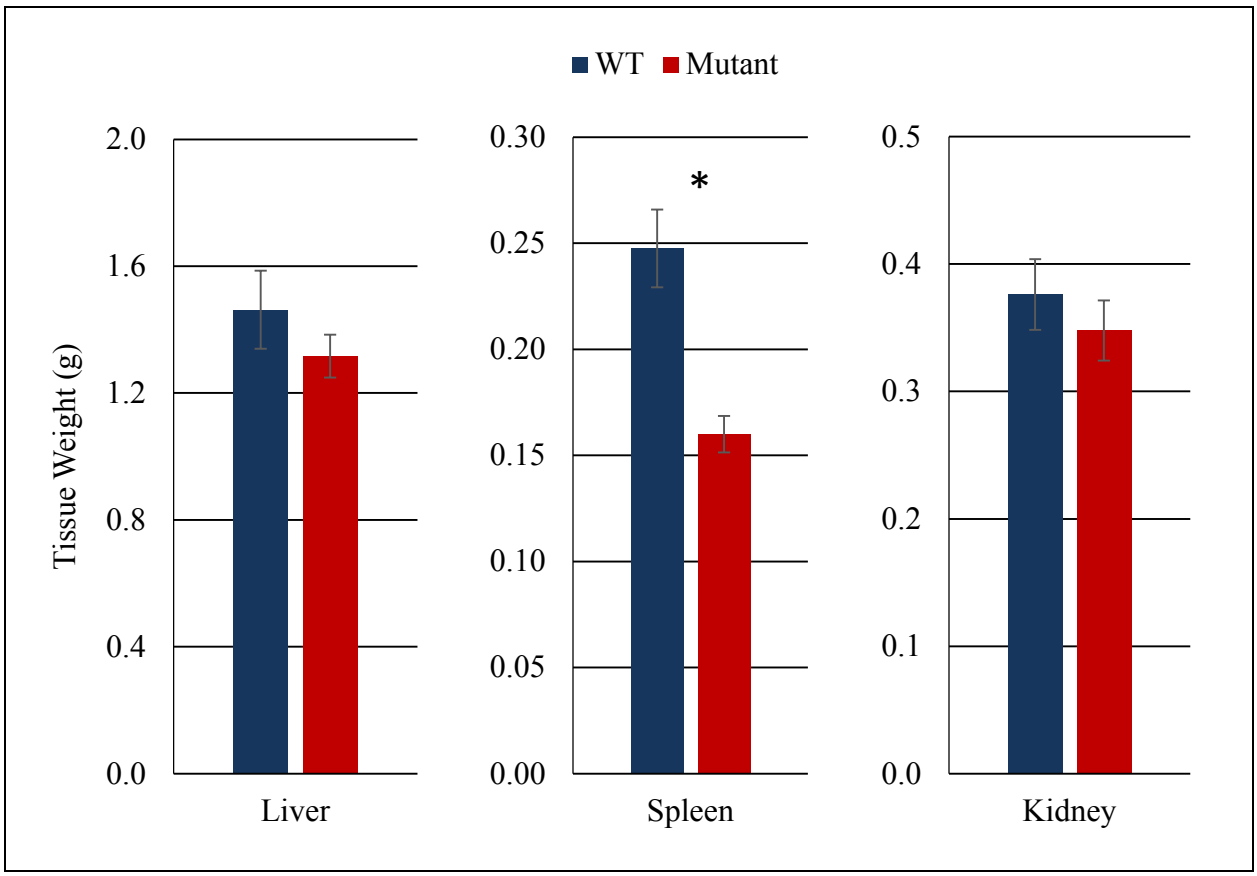

Figure 15: Tissue weight after secondary infection.

Tissue weights were measured on day 3 after secondary infection. Mutant and wild type mice showed no significant difference in liver or kidney weight. Mutant spleens were 35% smaller than wild type ($p<0.001$). Error bars indicate standard error. For liver and kidney, $n_{wt}=6$ $n_{mut}=5$. For spleen, $n_{wt}=12$ $n_{mut}=11$.

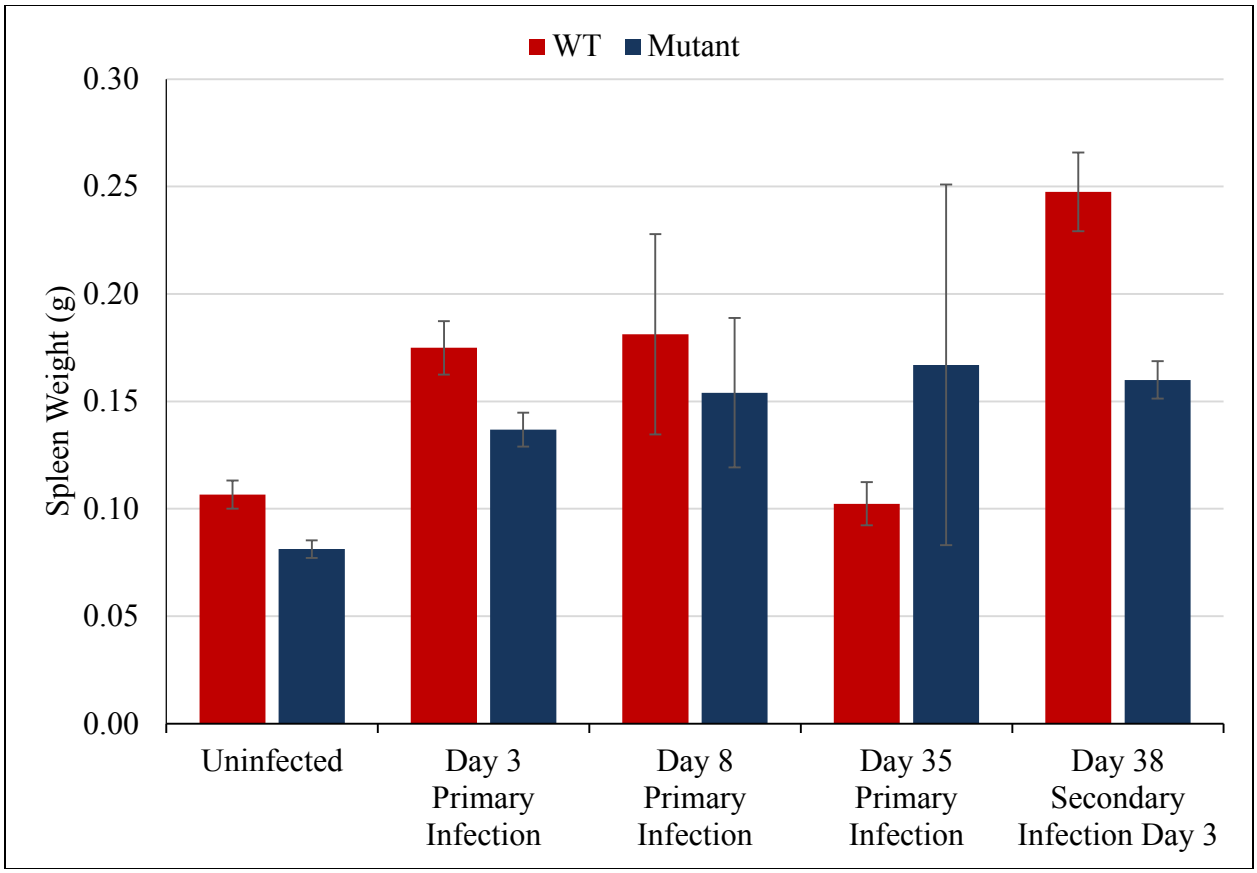

Figure 16: Spleen weight change at different stages of infection.

Mutant spleen weight is significantly smaller than wild type prior to infection, at day 3 after primary infection as well as at day 3 after secondary infection. Wild type spleens increase in size over the course of primary infection and return to baseline size by day 35. After secondary infection, wild type spleens quickly increase to their largest size. Mutant spleen weight is larger at day 3 after primary infection than prior to infection, however it remains unchanged after secondary infection compared to primary infection. Error bars indicate standard error. Refer to Table 5 for sample size for each group.

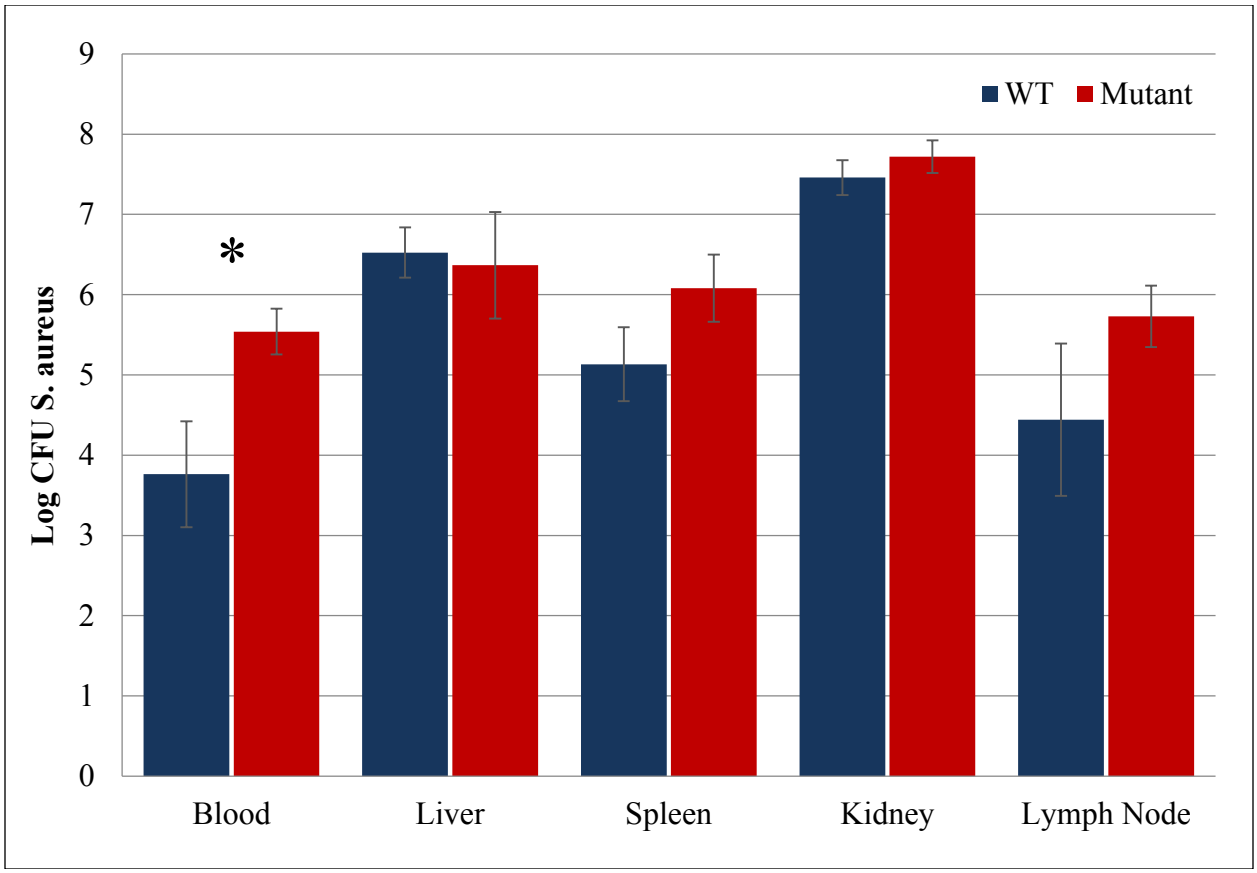

Figure 17: Bacterial load on day 3 after secondary infection.

Tissue samples tested 3 days after secondary infection show no difference in bacterial load between wild type and mutant mice in liver, spleen, kidney or lymph node. Mutant blood samples had significantly higher bacterial load than wild type ($p=0.045$). Results shown are CFU/mL for blood samples and CFU/g for liver, spleen, kidney and lymph node samples. Error bars indicate standard error. $n_{wt}=6$ $n_{mut}=6$.

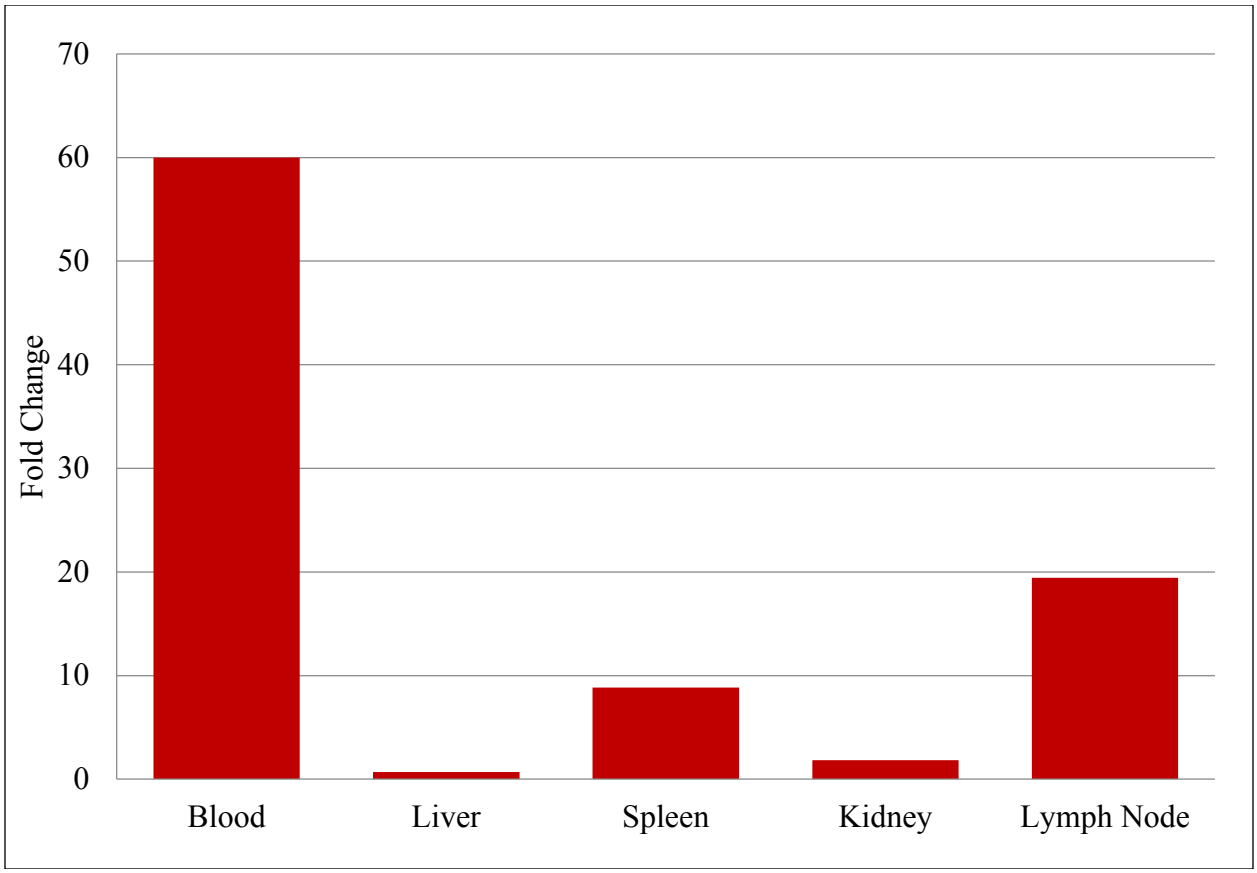

Figure 18: Mutant blood has 60 fold increase in bacterial load after secondary infection.

Average mutant bacterial load was divided by the average wild type bacterial load for each tissue, resulting in the fold change in bacterial load between wild type and mutant mice. Blood samples show a 60 fold increase in bacterial load of mutant blood compared to wild type ($p=0.045$). Changes in bacterial load in other tissues were not statistically significant. $n_{wt}=6$ $n_{mut}=6$.

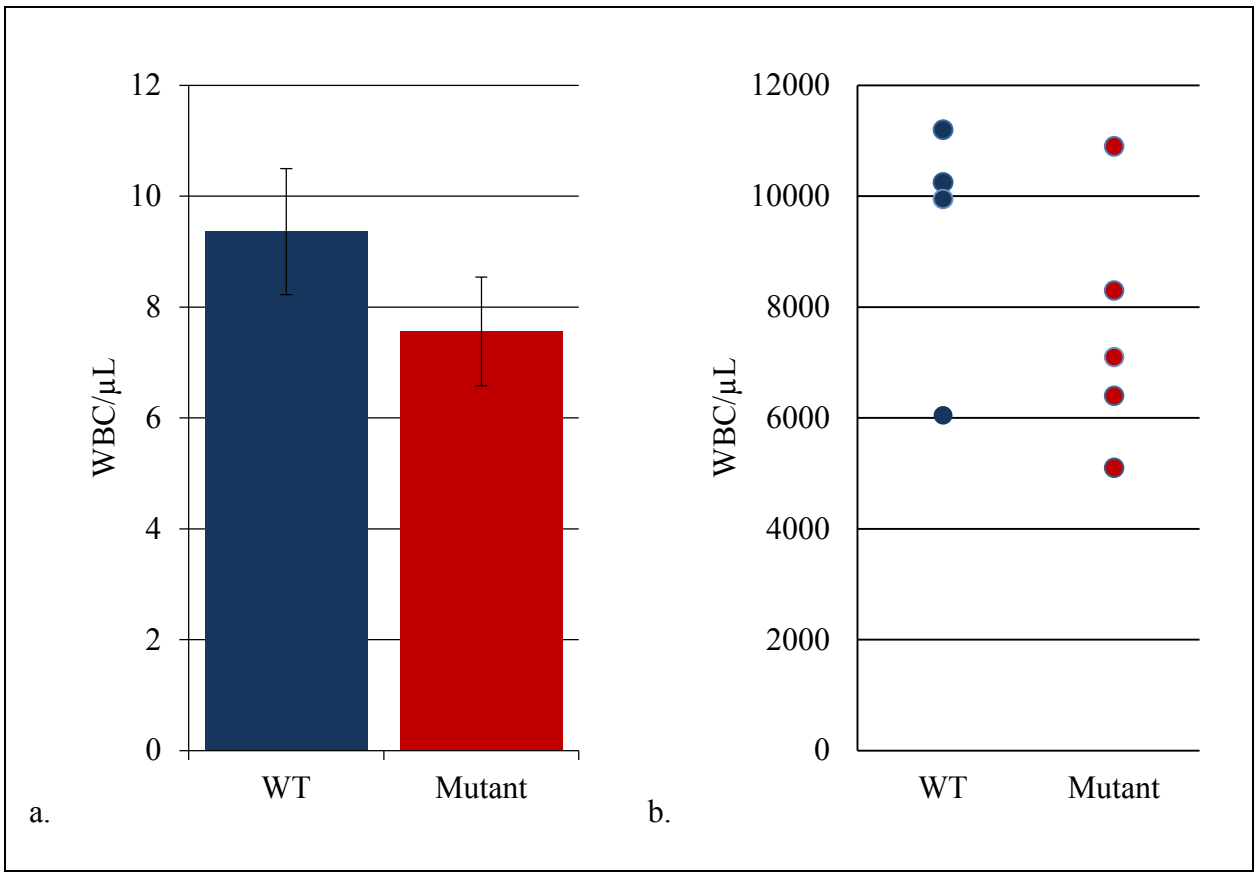

Figure 19: Secondary infection white blood cell counts.

Blood samples taken 3 days after secondary infection show no significant difference in white blood cell counts ($p=0.272$). (a.) Average white blood cell counts for wild type and mutant mice. Error bars indicate standard error. $n_{wt}=4$. $n_{mut}=5$. (b.) Dot plot showing individual samples. While this difference is not statistically significant, possibly due to the low sample size available, it is suggestive that there could possibly be a difference in the number of circulating lymphocytes. Values for both wild type and mutant samples are clustered together with one outlying sample each, thereby reducing the average difference between them.

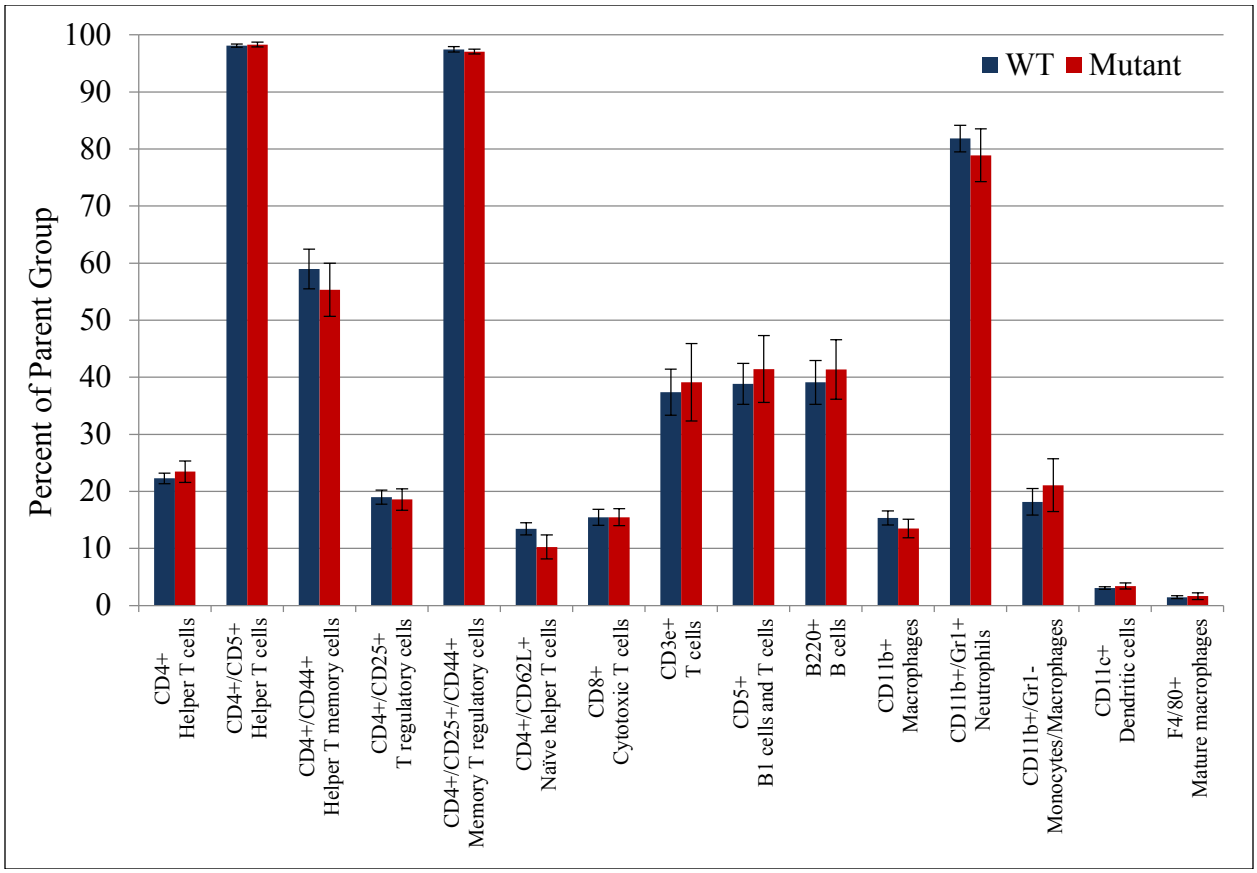

Figure 20: Lymphocyte populations in spleen on day 3 after secondary infection.

Spleen cell types were measured using flow cytometry on day 3 after secondary infection. No significant differences were observed between mutant and wild type for any of the cell types tested. Values shown are percent of total cells. Error bars indicate standard error. $n_{wt}=3$ $n_{mut}=3$. Values shown are percent of parent group. For example, CD4+ value is the percent of cells that are CD4+. CD4+/CD5+ value is the percent of CD4+ cells that are also CD5+.

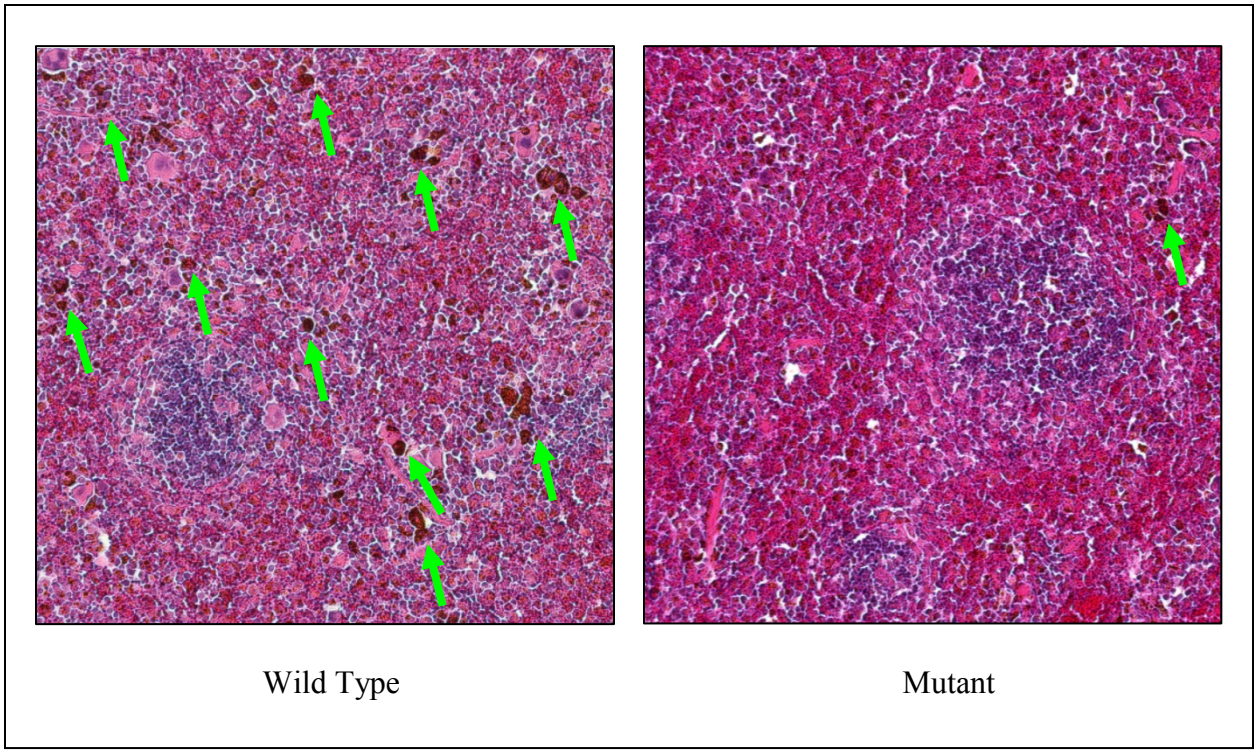

Figure 21: Secondary infection histology.

H&E stained paraffin sections of wild type and mutant spleens following secondary infection show lower levels of hemosiderin laden macrophages (indicated by green arrows) in mutant spleens than in wild type. This indicates that phagocytic function of splenic macrophages is reduced in mutant mice.

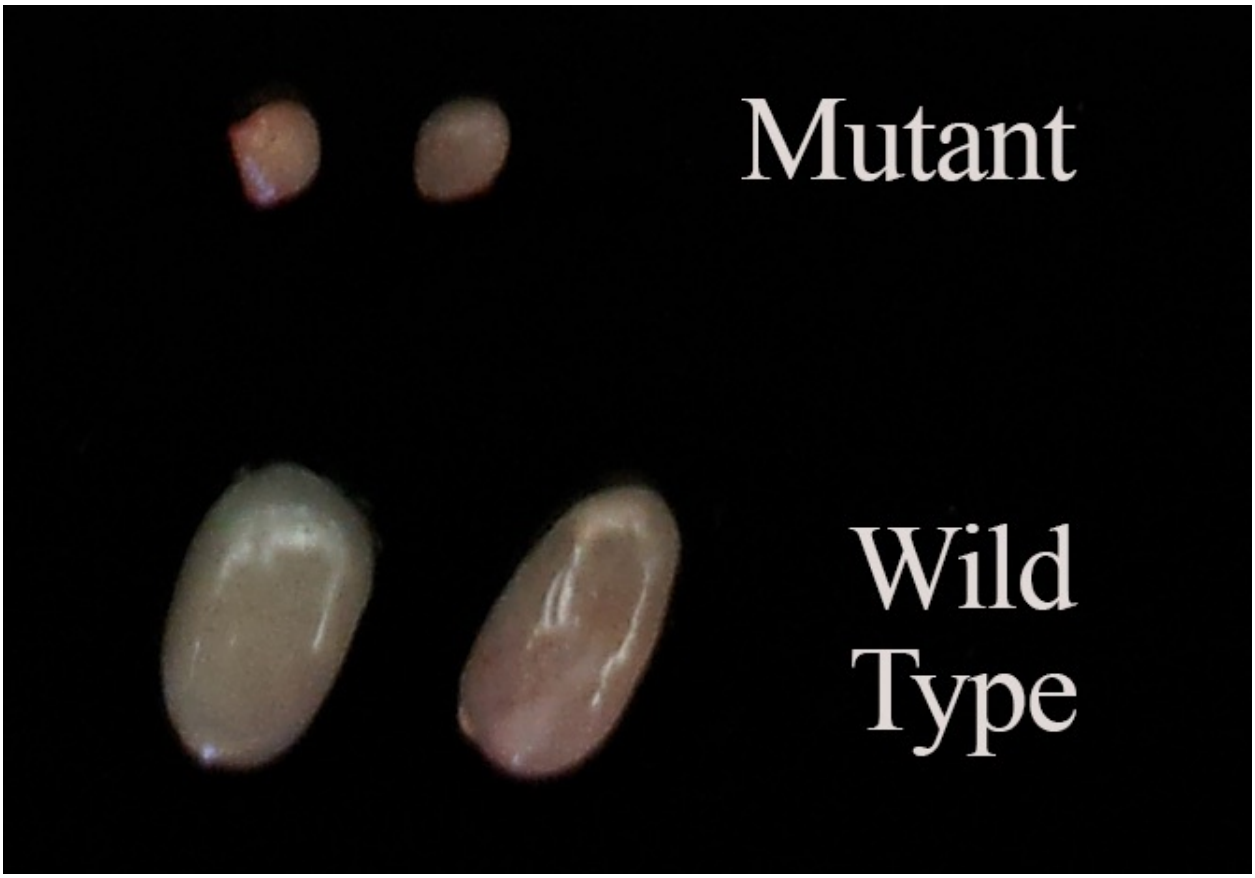

Figure 22: Lumbar lymph node size following secondary infection.

Representative samples of lumbar lymph node pairs from mutant and wild type mice 3 days after secondary infection. Lymph node enlargement after infection is typically due to accumulation and proliferation of lymphocytes. The failure of mutant lymph nodes to increase in size indicates that lymphocytes in the mutant mice have an impaired ability to respond to activation or migratory signals.

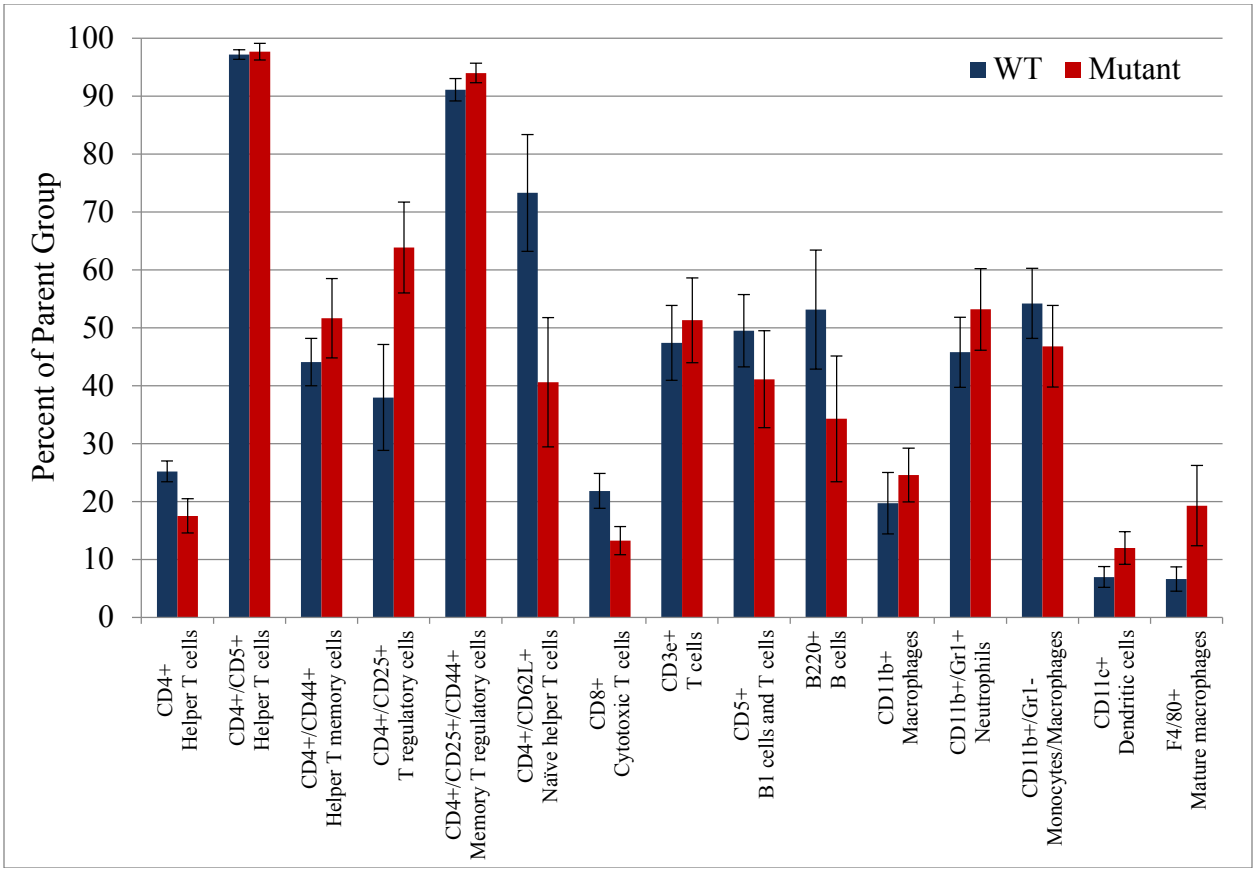

Figure 23: Lymphocyte populations in lymph node on day 3 after secondary infection.

Lymph node samples taken 3 days after secondary infection show significantly reduced levels of both $CD4^+$ ($p=0.033$) and $CD8^+$ ($p=0.040$) T-cells. Mutant $CD4^+$ levels are 70% of wild type and $CD8^+$ levels are 61%. $CD4^+/CD25^+$ ($p=0.064$) and $CD4^+/CD62L^+$ ($p=0.062$) T-cell subsets, as well as $F4/80^+$ ($p=0.144$) macrophages also show a possible difference between mutant and wild type. Error bars indicate standard error. $n_{wt}=5$. $n_{mut}=5$. Values shown are percent of parent group. For example, CD4+ value is the percent of cells that are CD4+. CD4+/CD5+ value is the percent of CD4+ cells that are also CD5+.

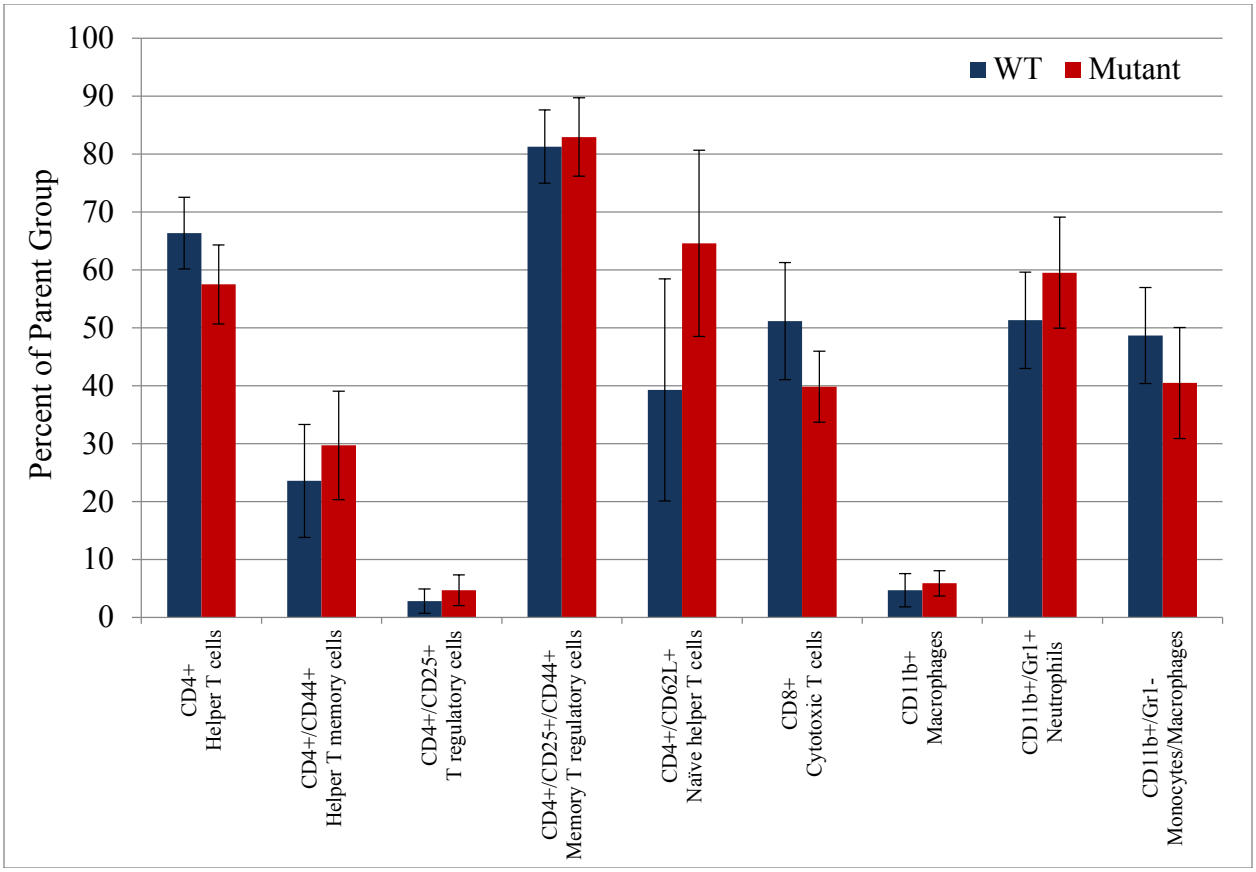

Figure 24: Lymphocyte populations in thymus on day 3 after secondary infection.

Thymus samples were taken 3 days after secondary infection and cell types were measured using flow cytometry. No significant differences were observed between mutant and wild type for any of the cell types tested. Error bars indicate standard error. n_{wt}=5. n_{mut}=5. Values shown are percent of parent group. For example, CD4+ value is the percent of cells that are CD4+. CD4+/CD5+ value is the percent of CD4+ cells that are also CD5+.

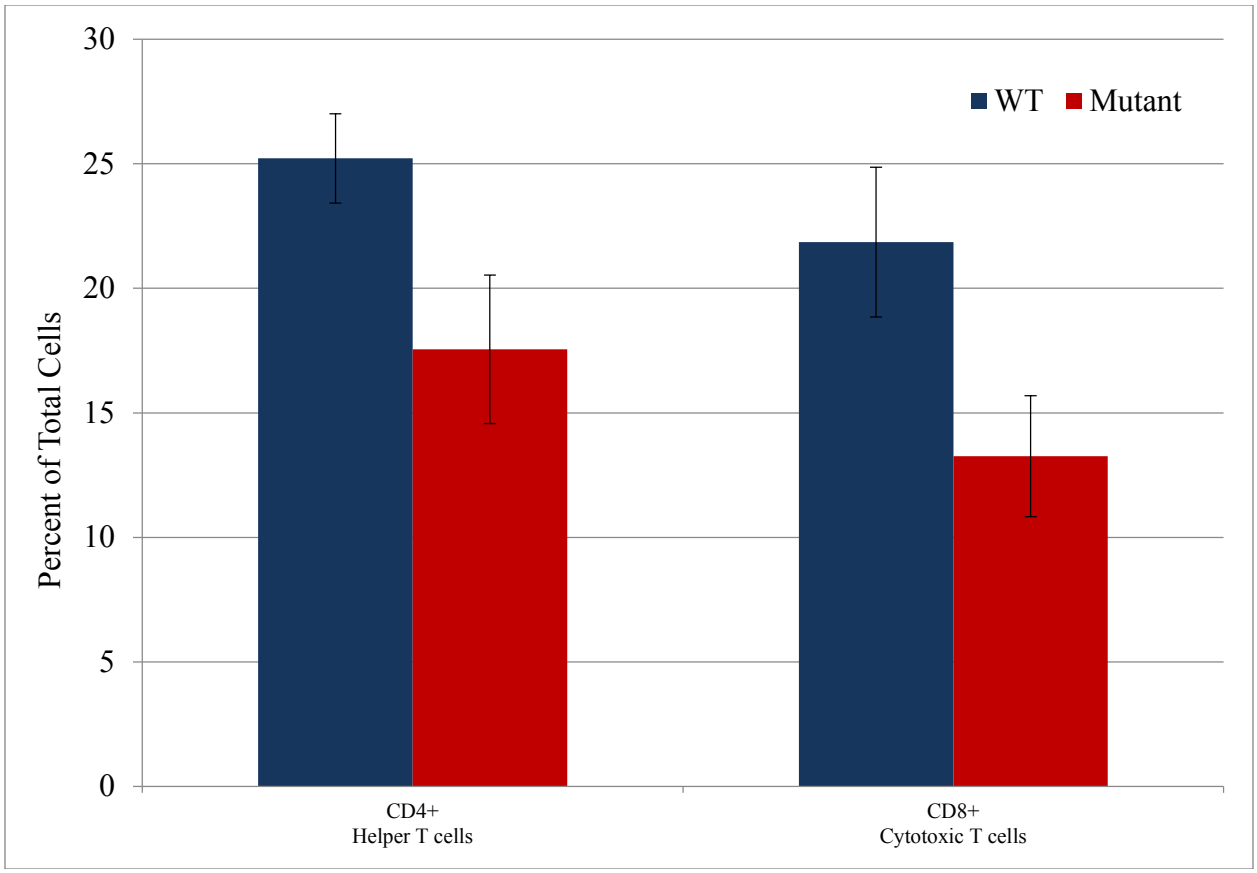

Figure 25: Lymph node T-cells after secondary infection.

Lymph node samples taken 3 days after secondary infection show significantly reduced levels of both $CD4^+$ ($p=0.033$) and $CD8^+$ ($p=0.040$) T-cells. Mutant $CD4^+$ levels are 70% of wild type and $CD8^+$ levels are 61%. Error bars indicate standard error. $n_{wt}=5$. $n_{mut}=5$.

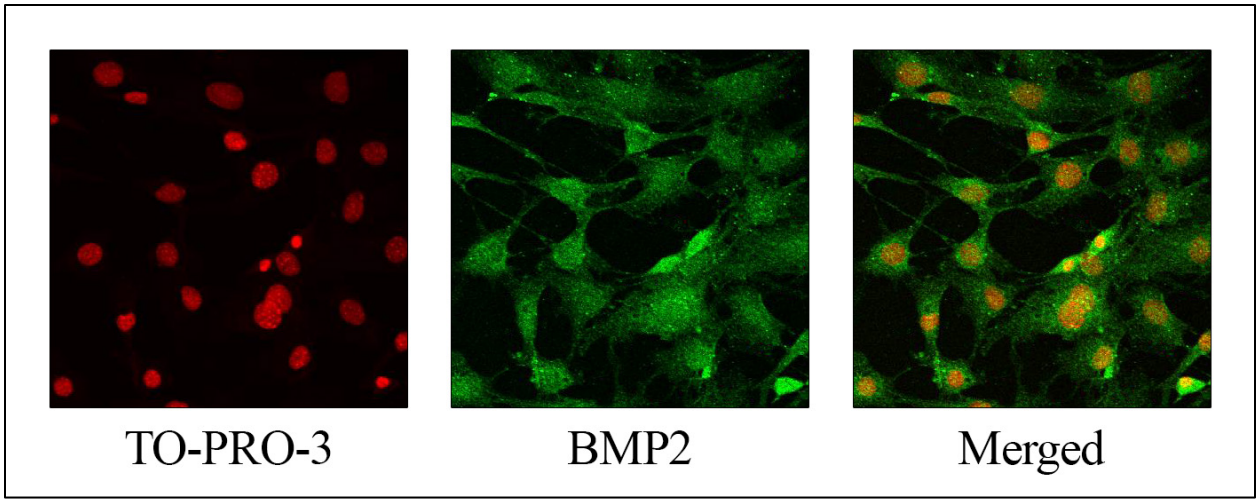

Figure 26: Immunofluorescent staining of HEK293 cells.

Cultured HEK293 cells show endogenous expression of nuclear BMP2. TO-PRO-3 was used to stain nuclei. BMP2 was stained using an Alexa Fluor® 488 conjugated antibody. Nuclear BMP2 is indicated by yellow areas in the merged image.

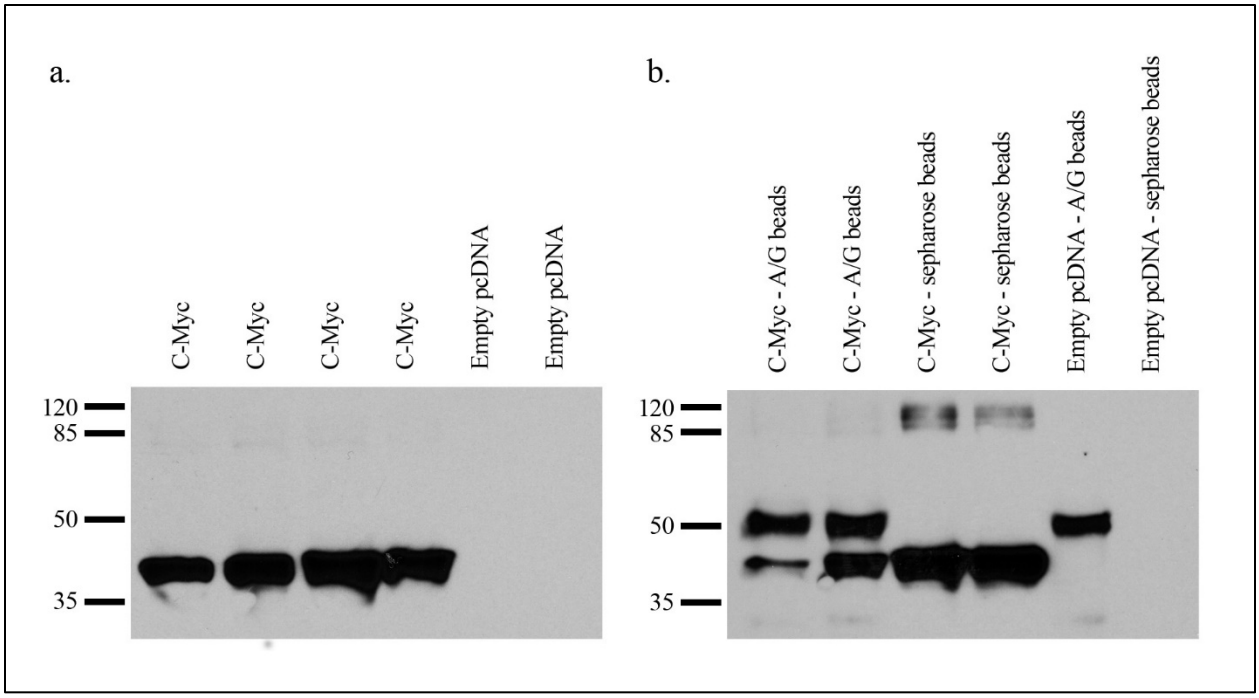

Figure 27: Western blot of Co-IP.

HEK293 cells were transfected with C-Myc-nBmp2. (a.) Cell lysate from transfected cells shows expression of nBMP2. (b.) nBMP2 remains after co-immunoprecipitation pull-down using both A/G and Myc-conjugated sepharose beads, indicating successful co-immunoprecipitation. Additional bands present are due to non-specific binding of secondary antibody to the beads.

1. Felin, J.E., et al., *Nuclear variants of bone morphogenetic proteins.* BMC Cell Biology, 2010. **11**.
2. Kingsley, D.M., *The TGF-beta superfamily: new members, new receptors, and new genetic tests of function in different organisms.* Genes & Development, 1994. **8**(2): p. 133-146.
3. Chen, D., M. Zhao, and G.R. Mundy, *Bone morphogenetic proteins.* Growth Factors, 2004. **22**(4): p. 233-241.
4. Christiansen, J.H., E.G. Goles, and D.G. Wilkinson, *Molecular control of neural crest formation, migration and differentiation.* Current Opinion in Cell Biology, 2000. **12**(6): p. 719-724.
5. Zhang, H. and A. Bradley, *Mice deficient for BMP2 are nonviable and have defects in amnion/chorion and cardiac development.* Development, 1996. **122**(10): p. 2977-86.
6. McCune, B.T., et al., *Binding of nBmp2 to PLSCR1 suggests a possible mechanism for nBmp2 regulation of Ca2+-modulating proteins.* The FASEB Journal, 2010. **24**(1_MeetingAbstracts): p. 833.20.
7. Schmidt, A.D., et al., *Mice bearing a targeted inactivation of nBmp2 show decreased muscle strength.* The FASEB Journal, 2009. **23**(1_MeetingAbstracts): p. 685.2.
8. Balschun, D., et al., *Deletion of the ryanodine receptor type 3 (RyR3) impairs forms of synaptic plasticity and spatial learning.* Embo Journal, 1999. **18**(19): p. 5264-5273.
9. Feske, S., *Calcium signalling in lymphocyte activation and disease.* Nature Reviews Immunology, 2007. **7**(9): p. 690-702.
10. Lewis, R.S., *Calcium signaling mechanisms in T lymphocytes.* Annual Review of Immunology, 2001. **19**: p. 497-521.
11. Vig, M. and J.P. Kinet, *Calcium signaling in immune cells.* Nature immunology, 2009. **10**(1): p. 21-27.
12. Baba, Y. and T. Kurosaki, *Impact of Ca2+ signaling on B cell function.* Trends in Immunology, 2011. **32**(12): p. 589-594.
13. Cesta, M.F., *Normal structure, function, and histology of the spleen.* Toxicologic Pathology, 2006. **34**(5): p. 455-465.
14. Mori, Y., et al., *Transient receptor potential 1 regulates capacitative Ca2+ entry and Ca2+ release from endoplasmic reticulum in B lymphocytes.* Journal of Experimental Medicine, 2002. **195**(6): p. 673-681.
15. Alexander, E.L. and B. Wetzel, *Human Lymphocytes - Similarity of B and T Cell Surface Morphology.* Science, 1975. **188**(4189): p. 732-734.
16. Oh-Hora, M. and A. Rao, *Calcium signaling in lymphocytes.* Current Opinion in Immunology, 2008. **20**(3): p. 250-258.
17. Robert, V., et al., *Calcium signalling in T-lymphocytes.* Biochimie, 2011. **93**(12): p. 2087-2094.
18. Grigg, J.C., et al., *Structural biology of heme binding in the Staphylococcus aureus Isd system.* Journal of Inorganic Biochemistry, 2010. **104**(3): p. 341-348.

19. Nilsson, I.M., et al., *Alpha-toxin and gamma-toxin jointly promote Staphylococcus aureus virulence in murine septic arthritis.* Infection and Immunity, 1999. **67**(3): p. 1045-1049.
20. Kobayashi, S.D., et al., *Rapid Neutrophil Destruction following Phagocytosis of Staphylococcus aureus.* Journal of Innate Immunity, 2010. **2**(6): p. 560-575.
21. Liu, G.Y., *Molecular Pathogenesis of Staphylococcus aureus Infection.* Pediatric Research, 2009. **65**(5): p. 71R-77R.
22. Berger, M., et al., *Calcium Requirements For Increased Complement Receptor Expression During Neutrophil Activation.* Journal of Immunology, 1985. **135**(2): p. 1342-1348.
23. Lindemann, O., et al., *TRPC6 Regulates CXCR2-Mediated Chemotaxis of Murine Neutrophils.* The Journal of Immunology, 2013. **190**(11): p. 5496-5505.
24. Kudo, F., et al., *Neutrophil phagocytosis is down-regulated by nucleotides until encounter with pathogens.* Immunology Letters, 2012. **144**(1-2): p. 24-32.
25. Rakhmilevich, A.L., *Neutrophils are essential for resolution of primary and secondary infection with Listeria monocytogenes.* Journal of Leukocyte Biology, 1995. **57**(6): p. 827-831.
26. Teixeira, F.M., et al., *Staphylococcus aureus infection after splenectomy and splenic autotransplantation in BALB/c mice.* Clinical and Experimental Immunology, 2008. **154**(2): p. 255-263.
27. William, B.M., et al., *Hyposplenism: A comprehensive review. Part II: Clinical manifestations, diagnosis, and management.* Hematology, 2007. **12**(2): p. 89-98.
28. William, B.M. and G.R. Corazza, *Hyposplenism: A comprehensive review. Part 1: Basic concepts and causes.* Hematology, 2007. **12**(1): p. 1-13.
29. Trigg, M.E., *Immune Function of the Spleen.* Southern Medical Journal, 1979. **72**(5): p. 593-599.
30. Price, V.E., et al., *The prevention and treatment of bacterial infections in children with asplenia or hyposplenia: Practice considerations at the Hospital for Sick Children, Toronto.* Pediatric Blood & Cancer, 2006. **46**(5): p. 597-603.
31. Bohnsack, J.F. and E.J. Brown, *The Role of the Spleen in Resistance to Infection.* Annual Review of Medicine, 1986. **37**: p. 49-59.
32. Hansen, K. and D.B. Singer, *Asplenic-hyposplenic overwhelming sepsis: Postsplenectomy sepsis revisited.* Pediatric and Developmental Pathology, 2001. **4**(2): p. 105-121.